PCCP

Dynamic Article Links ►

Cite this: DOI: 10.1039/c0xx00000x

www.rsc.org/xxxxxx

PERSPECTIVE

The roughness of the protein energy landscape results in anomalous diffusion of the polypeptide backbone†

Martin Volk,*[a] Lilia Milanesi,[b] Jonathan P. Waltho,[c,d] Christopher A. Hunter,[e] Godfrey S. Beddard[f]

Received (in XXX, XXX) Xth XXXXXXXXX 20XX, Accepted Xth XXXXXXXXX 20XX

DOI: 10.1039/b000000x

Although protein folding is often described by motion on a funnel-shaped overall topology of the energy landscape, the many local interactions that can occur result in considerable landscape roughness which slows folding by increasing internal friction. Recent experimental results have brought to light that this roughness also causes unusual diffusional behaviour of the backbone of an unfolded protein, *i.e.* the relative motion of protein sections cannot be described by the normal diffusion equation, but shows strongly subdiffusional behaviour with a nonlinear time dependence of the mean square displacement, $\langle r^2(t)\rangle \propto t^{\alpha}$ ($\alpha << 1$). This results in significantly slower configurational equilibration than had been assumed hitherto. Analysis of the results also allows quantification of the energy landscape roughness, *i.e.* the root-mean-squared depth of local minima, yielding a value of 4-5 k_BT for a typical small protein.

Introduction

Proteins are involved in virtually all biological processes and perform a multitude of functions, including scaffolding, sensing, signalling, transport, energy conversion and catalysis of chemical reactions. The particular function which a protein has is defined by its three-dimensional shape, which in many cases is determined fully by its primary structure (the exact sequence of amino acids from which the protein has been built following the instructions stored in the genetic code).[1] Whereas the translation of the genetic code, *i.e.* the controlled synthesis of the protein on the ribosome, is reasonably well understood, many questions remain about the process by which the newly synthesised protein folds into its highly organised functional three-dimensional structure. As originally pointed out by Levinthal,[2] because of the large number of possible conformations which are accessible even to a small protein, it is impossible for protein folding to occur by a random search through conformational space. Instead, there must be some inherent "instructions" or principles which efficiently guide the folding protein towards its native functional state in spite of the complexity of the process. Full elucidation of these principles remains the basic aim of protein folding research.

In recent years, the concept of motion on a (multidimensional) energy landscape[3-6] has been used increasingly to describe the dynamics of protein folding and smaller structural changes occurring during the normal function of the protein, such as ligand binding. This landscape is given by the energy of the protein as a function of the many coordinates describing the protein's conformation, which include the backbone dihedral bond angles, but also the side chain coordinates which play an important role especially for more compacted states. Under folding conditions, the landscape has an overall funnel-like topology,[7] which directs the folding protein to the native structure, Fig. 1A.‡ However, this funnel-shaped surface is not smooth, but highly corrugated (other terms used in this context are "rugged" or "rough") due to the multitude of potential local interactions which affect the energy of the protein and can temporarily trap it in a non-native local conformation. The relevant interactions include attractive and repulsive backbone and side chain interactions, but other effects, such as dihedral rotational energies or the energetic cost of creating voids within the protein, also contribute. The wide range of interaction strengths encountered in proteins and cooperative effects lead to a hierarchy of well depths on different energy and length scales,[3] as schematically indicated in Fig. 1B. The folding process can be described as motion on this multidimensional rough surface towards the bottom of the funnel. Since the surface is corrugated, motion on the surface is not uniform in time as barriers of different heights need to be crossed. Furthermore, the exact pathway taken by the protein depends not only on the starting position on the landscape, *i.e.* its initial conformation, but will also be subject to statistical fluctuations due to the existence of different escape routes from any local minimum, and hence each protein takes one of a multitude of potential routes during folding, as indicated in Fig. 1A. Thus, there is no microscopic folding mechanism in the sense of a reaction mechanism as used in chemistry.

The heights of the barriers between local wells, *i.e.* the roughness of the energy landscape, determine the effective speed of motion through conformational space, and hence the time scale of folding or other structural changes. In this context, the notion of "internal friction" is often used to describe the contribution of the energy landscape roughness to the slowing of conformational changes,[8-11] which occurs in addition to the friction arising from solvent viscosity. The term "internal friction" may be somewhat misleading, since the interactions defining the rough energy

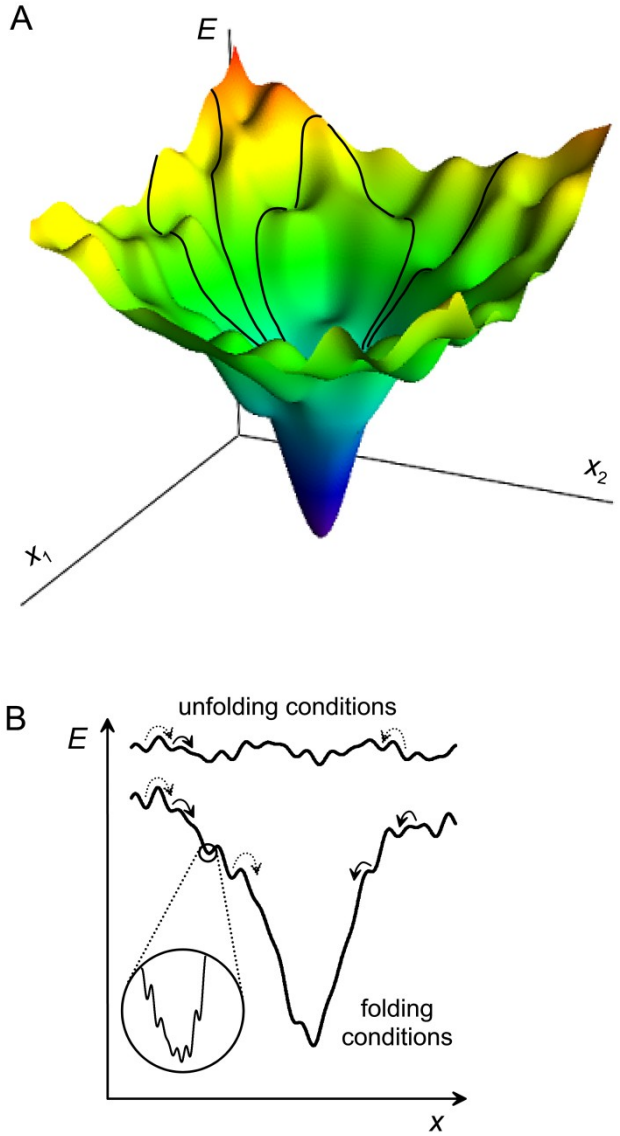

Fig. 1 Multidimensional rugged energy landscape, shown schematically for two (A) or one (B) of the many coordinates required to specify a protein's conformation. (A) Two-dimensional cartoon of the folding funnel; shown is the energy, E, plotted against two conformational coordinates, x_1 and x_2;[‡] the black lines on the energy surface indicate different possible folding pathways. (B) One-dimensional representation of the energy landscape under folding or unfolding conditions, respectively, showing local minima with short (solid arrows) or long (dotted arrows) trapping times. The inset of (B) shows the hierarchy of well depths on different energy and length scales. It should be noted that, although shallower wells may exist, only wells with depths comparable to or greater than thermal energies, k_BT, where k_B is Boltzmann's constant and T the absolute temperature, are of relevance, since only these lead to significant trapping.

landscape are not exclusively intra-protein, but also include protein-solvent interactions, which have been shown to be of great importance for protein dynamics and function.[6,12] Hence, energy landscape roughness, and therefore "internal friction", may depend on solvent conditions. In fact, denaturants have been shown to reduce the strength of intra-peptide interactions and thereby reduce energy landscape roughness and internal friction,[13-22] whereas there are indications that an increase of temperature leads to increased roughness due to the increasing strength of the hydrophobic effect.[23-27]

Seemingly in contrast to this kinetic complexity of folding on a rough funnel-shaped energy landscape, many proteins have been shown experimentally to follow two-state folding, *i.e.* the relaxation between the manifold of unfolded conformations and the much better-defined folded state upon a fast change of equilibrium conditions follows an exponential time dependence. In terms of energy landscape theory, this is expected if the *free* energy profile along some suitable reaction coordinate(s) is dominated by two minima separated by a barrier. It should be noted that the free energy profile is, in effect, a projection of the multidimensional energy surface that also takes into account entropy, *i.e.* the number of conformations for a particular value of the reaction coordinate. Therefore, the barrier arises from an intricate interplay of entropy and energy and may not relate to an individual actual barrier on the multidimensional energy landscape.[5,28] The free energy profile may display some roughness, but this is not the same as the roughness of the underlying full multidimensional energy landscape and depends on the choice of reaction coordinate,[29,30] since each point on the free energy profile corresponds to an average over the many conformations yielding this particular value of the reaction coordinate. Nevertheless, the roughness of the multi-dimensional energy landscape affects the speed of conformational changes and hence determines the speed of motion along the reaction coordinate, and thus the pre-exponential factor for the folding rate constant. According to Kramers' theory, it also will influence the speed of motion through the transition state,[11] which has been experimentally observed to decrease at higher temperatures, most likely due to stronger internal friction as a result of increased energy landscape roughness.[26,27] Motion on a rough energy landscape has also been directly implicated in the observation of "strange" (*i.e.* non-exponential) kinetics of protein folding in the absence of a significant barrier.[23,31]

In this Perspective, we first review previous experimental approaches which aim to elucidate the speed of motion over the rough protein energy landscape. Most of these experiments observe the diffusive motion of specific residues, and have yielded significant insight into the dynamics of the polypeptide backbone. However, in only a few cases was an attempt made to quantify landscape roughness from the results. Similarly, mechanical unfolding experiments on single proteins have been used to obtain a quantitative characterisation of the roughness. We then describe a recently reported alternative approach for the experimental characterisation of backbone dynamics and energy landscape roughness.[32] Most interestingly, these results show that the polypeptide backbone does not follow normal diffusional behaviour, but undergoes subdiffusional motion due to a wide range of trapping times arising from the hierarchy of local energy minima on the rough energy landscape. Analysis of the experimental observations allows a quantitative determination of the roughness. Finally, we discuss some potential consequences of the observed anomalous diffusional behaviour of the backbone for protein folding and give an outlook on future work which will make use of the new method.

Backbone Dynamics Investigated by Loop Formation Experiments

Principle of the Method

Motion over the rough energy landscape of unstructured peptides lacking deep traps, in particular intrachain diffusion[§] resulting in loop formation, has been studied extensively on the nano- to microsecond time scale, mainly using fluorescence and triplet quenching.[33] Loop formation is of high interest in the context of protein folding since it is a pre-requisite for the formation of native contacts, and thus often is regarded as the first step of folding.

The principle of the loop formation method is shown in Fig. 2. A reporter group within a peptide or protein is excited by a short laser flash and the decay of the excited singlet or triplet state is followed by time-resolved spectroscopy. In the presence of another group on the backbone which quenches this excited state upon contact formation,[¶] the lifetime of the excited reporter state is reduced if significant intra-chain loop formation occurs on the relevant time scale. Thus, analysis of the observed quenching dynamics allows the observation of loop formation dynamics, which not only is directly relevant for the formation of secondary and tertiary structures, but also provides more general information on polypeptide backbone dynamics. The time scale of the method is limited by the intrinsic lifetime of the reporter state in the absence of quenching, which is typically on the 1-10 microsecond time scale.

Ligand rebinding experiments in heme proteins after photolysis of CO work on a similar principle, although the reporter state (*i.e.* the ligand-free heme) does not get permanently deactivated by loop formation, but only by CO-rebinding, so that the time window is extended to the sub-ms-range.[34]

In a related approach, single molecule fluorescence correlation techniques[35] are employed with short-lived fluorescence reporter states whose fluorescence is quenched when in contact with a quencher group[36] or by fluorescence resonance energy transfer (FRET) if a suitable acceptor is nearby.[15,37] In these experiments, conformational or loop formation dynamics are measured using the time correlation of fluorescence photons from single proteins instead of ensemble quenching kinetics. The intrinsic fluorescence lifetime on the ns-time scale defines the lower limit of the time window accessible by these experiments, whereas translational diffusion of the single molecule out of the observation volume on the sub-ms-time scale gives the maximum upper limit, although often triplet dynamics limit the applicable time window to the microsecond range. Only recently, this time window could be extended to 100 ms by observing repeated returns of single molecules to the observation volume.[38]

Unstructured Peptides

Single exponential decay of the reporter state due to loop formation was found on the time scale of tens of nanoseconds to microseconds in oligopeptides lacking significant intra-peptide interactions or secondary structure,[13,39-56] which was taken as indication for fast conformational equilibration of such peptides on these time scales.[57] More complex and non-exponential quenching dynamics were observed on the ns- and sub-ns time scale[52,58] due to incomplete conformational averaging on such short time scales, so that the motion of the backbone is limited to local basins of the rough energy landscape.

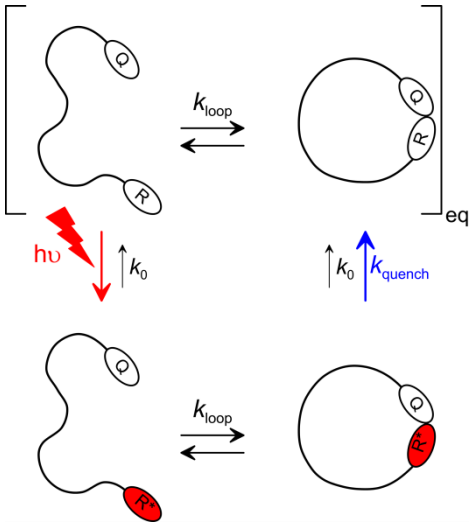

Fig. 2 Principle of the loop formation method for observing backbone dynamics. The polypeptide backbone is in equilibrium between all accessible conformations at all times; this includes looped conformations in which the reporter group (R) and the quencher (Q) are in contact (right), but it is reasonable to assume that in most conformations they are at a significant distance from each other (left). A short laser pulse (hν) excites R to the reporter state (R*, shown in red); excitation in looped conformations normally leads to immediate de-excitation, and thus is not included here for simplicity. The reporter state decays back to the ground state with its intrinsic decay rate constant, k_0, typically on the nano- to microsecond time scale. Loop formation with rate constant k_{loop} leads to contact with the quencher and deactivation of R* with rate constant k_{quench}; the reduced lifetime of the reporter state thus allows quantification of k_{loop}.

These experimental results on unstructured peptides provide quantitative information on the intrinsic dynamics of the polypeptide backbone in the absence of strong local traps caused by side chain interactions, *i.e.*, for motion on a relatively smooth potential energy landscape. In particular, the experimentally observed dependence of loop formation dynamics on the length of the backbone, N, is in agreement with theoretical considerations; the rate constant for loop formation, k_{loop}, was found to be almost independent of the chain length for peptides with only a few residues due to chain stiffness and/or residual interactions (*vide infra*) and to approach $k_{loop} \sim N^{1.5}$ - $N^{1.8}$ for longer peptides,[39,40,43-45,48-50,53,56] which is in agreement with the simplest models for polymer loop formation dynamics, although more advanced theories and modelling tend to predict a slightly stronger power dependence.[57,59,60] Significant effects of the amino acid content on the polypeptide dynamics of heteropeptides were only observed for the highly flexible glycine and the stiff proline,[43-48,52,55] whereas somewhat larger variations were found for homopeptides.[41,54] Loop formation between interior residues is somewhat slower than loop formation between the backbone ends, which was ascribed to the decreased flexibility of interior residues and excluded volume effects,[49,51] although other effects, such as residual structure, may also play a role.[60,61] Interestingly, the loop formation rates for β-peptides were found to be similar to those for α-peptides with the same number of residues in spite of their larger contour length, which was ascribed to the increased conformational flexibility of β-peptides arising from the additional methylene group in the backbone.[48] On the other hand, glycosylated peptides have slower loop formation dynamics.[62]

As noted above, the speed of peptide segment diffusion is governed by two main effects, namely solvent friction, *i.e.* the viscosity of the solvent through which the peptide chain moves, and internal friction, *i.e.* retardation of peptide segment motion arising from peptide internal interactions, which is directly related to the roughness of the local energy landscape. The influence of solvent friction manifests itself in the viscosity dependence of the loop formation rate of unstructured peptides,[39,40,42,47,49,53,55,62] in particular the different rates found in H_2O and D_2O which have significantly different viscosity.[46,58]

On the other hand, a significant contribution from internal friction, *i.e.* significant residual interactions, was suggested even for short unstructured peptides by the temperature dependence of k_{loop}, which is more pronounced than expected from solvent viscosity alone.[46,49,50,58] In agreement with this conclusion, the presence of denaturants was found to lead to faster backbone diffusion in spite of higher solvent viscosity[13] and to a more ideal dependence of the loop formation rate on peptide length;[45,49] both of these observations point to the suppression of interactions such as hydrogen bonding or the hydrophobic effect by the denaturant. On the other hand, the same effect leads to an increase in the equilibrium chain dimensions upon addition of denaturant,[13,49,55] resulting in overall slower loop formation,[41,42,45,46,48,49,55] and some models suggest that this, rather than internal friction, is the main effect of denaturants on the loop formation dynamics of the simplest peptides with only weakly interacting side chains.[63] On the other hand, the presence of backbone hydrogen bonds in unstructured peptides, resulting in faster loop formation due to a restricted conformational space, has recently been confirmed by Molecular Dynamics (MD) simulations[56] and experiments on modified peptides unable to form such hydrogen bonds.[64] Finally, molecular crowding at a level comparable to that found in the cellular environment was shown to not significantly affect loop formation rates for unstructured peptides; this is due to the reduced conformational space available to the peptide in a highly crowded environment, which counteracts the slower translational diffusion in such an environment.[53]

These experiments also yield empiric values for the effective intrapeptide diffusion constant for relative motion of peptide segments, if the mean square end-to-end distance, $\langle r^2 \rangle$, can be modelled or measured directly. At room temperature, values of ~4 Å^2/ns were found in the absence of denaturant,[13,43] increasing to ~8-27 Å^2/ns in the presence of high concentrations (several M) of denaturant.[13,37]

Peptides with Secondary Structure and Proteins

Double-exponential quenching dynamics of the reporter state were found on the time scale of 10-100 ns in alanine-based α-helical model peptides,[65,66] which gave elegant access to helix-coil transition dynamics under equilibrium conditions; the results were found to be in good agreement with helix-coil relaxation dynamics observed under non-equilibrium conditions.[67-72] The conformational dynamics of the unfolded peptide sections, on the other hand, were found to be similar to those observed in the unstructured peptides discussed above.[66]

In a similar manner, the same techniques could be applied to small proteins, naturally occurring peptides or protein fragments.[14-22,34,37,64,73-86]. Under conditions of marginal stability, these experiments yield the backbone dynamics of the unfolded state, as well as the dynamics of the folding reaction under equilibrium conditions, if these occur within the accessible time window. The folding dynamics observed in these experiments are close to the results of more traditional non-equilibrium methods,[76,79,82,84] in agreement with the fluctuation-dissipation theorem. More interestingly, loop formation or backbone reconfiguration dynamics of the unfolded state could be determined under solvent conditions that favour folding in marginally stable proteins,[15,17,22,79,83,86] in proteins unfolded by introducing mutations,[18,64,79,82] in intrinsically denatured proteins,[19,64,77,78,80,81,85,86] or in a rapid mixer setup which allows observation of an unfolded protein ensemble under folding conditions before folding occurs after changing solvent conditions.[20-22,86] These experiments show that in the absence of denaturant the unfolded state of a real protein often has significantly slower intrapeptide diffusion and consequently loop formation than simple oligopeptides of similar size, indicating increased internal friction due to side chain interactions. This conclusion is further confirmed by the viscosity dependence of the loop formation dynamics in unfolded proteins, which extrapolates to a significant loop formation time even for zero solvent viscosity,[18,22,79,85,86] similar to the viscosity dependence of the folding rate of fast folding proteins [10,11,26] or that of protein conformational changes;[9] interestingly, proteins which fold on time scales of milliseconds or slower normally do not show such behaviour and thus seem to be dominated by solvent friction, although recently some exceptions have been reported.[87] Furthermore, it was found that the activation energy of loop formation is significantly higher than expected from the temperature dependence of solvent friction alone.[74,79] The addition of denaturants speeds up backbone motion and loop formation to much larger extent than for simple model peptides,[14-22] in spite of the increased viscosity and the larger chain dimensions adopted under such conditions.[15,21,22,80,86,88] Both of these observations yield further confirmation of the presence of internal friction and transient structure due to side chain interactions which are greatly reduced in the presence of denaturants.

Diffusion constants of fully unfolded protein segments in the presence of denaturant were found to be of similar size as the values for unstructured peptides mentioned above, *i.e.* 2-20 Å^2/ns, but diffusion slows down significantly under conditions where the protein collapses or even adopts structure with marginal or significant stability.[15-17,19-21,37,73,77,85] A similar conclusion was drawn from the temperature-dependent dynamics of the hydrophobic collapse of an unfolded protein.[24]

Thus, important information on polypeptide backbone motion on the rough energy landscape has been gained with these methods. However, it should be noted that the time scale accessible by quenching methods is limited by the lifetime of the reporter state, which is typically of the order of microseconds. Single molecule fluorescence correlation techniques extend this time window, but still are limited to sub-millisecond time scales. Furthermore, the polypeptide backbone normally is in conformational equilibrium in these experiments, so that only lower lying sections of the energy landscape are accessed. This constitutes another limitation of the loop formation methods, since it has been shown that internal friction may vary

significantly over the landscape or along the reaction coordinate.[22,29,30]

Energy Landscape Roughness

A few of the reports described above attempted to estimate the roughness of the energy landscape underlying the observed diffusional motion, *i.e.* the root-mean-squared depth of local minima. All of these estimates are based on Zwanzig's theory of the slowing of motion in a rough potential,[89] although it is not clear *a priori* to what extent this one-dimensional treatment is applicable to motion on a multi-dimensional energy landscape or how the roughness of the underlying multidimensional energy landscape affects diffusion of polypeptide backbone segments in three-dimensional space; recently, some doubt has been raised about the applicability of one-dimensional models for describing certain aspects of polymer conformational changes.[90,91] Furthermore, it is difficult to estimate the relevant diffusion constants in the absence of roughness which are required for estimating the effect of roughness from experimentally observed diffusion constants.[92] For unstructured peptides, a roughness of ~ 1.7 k_BT (where k_B is the Boltzmann constant and T the temperature) was suggested from the slower diffusion of the peptide end groups compared to free molecules of similar size.[43] Similarly, the slow backbone diffusion of protein L in the absence of denaturant, when compared to diffusion of the overall protein, predicted a roughness of ~ 2.6 k_BT.[20] Finally, a decrease of the energy landscape roughness by ~ 1.3 k_BT upon addition of denaturant at high concentrations was found for cold shock protein.[15]

These values are in broad agreement with estimates obtained from experimental results of protein folding kinetics. Thus, a lower limit of 0.8 k_BT for the energy landscape roughness was estimated for the β-hairpin peptide trpzip2 from the different kinetics found with different probes.[93] A roughness of 0.8 k_BT was suggested for the five-helix bundle protein $\lambda_{6\text{-}85}$ by an analysis of the fast ("molecular") phase of its folding kinetics using Langevin simulations,[25] whereas a roughness of 1.9 k_BT is suggested by the reduced diffusion coefficient estimated from similar data[94] when applying Zwanzig's theory.[89] Comparative studies on a three-helix-bundle protein family indicated a variation of roughness by up to 2 k_BT within this protein family.[87]

Measuring Energy Landscape Roughness Using Mechanical Unfolding

The unfolding of single molecules by the application of an external force provides an alternative experimental approach to measuring the roughness of a protein's energy landscape. In these experiments, two contact points on a single protein are pulled apart using optical tweezers or an Atomic Force Microscope (AFM), resulting in force-induced unfolding of the protein, the dynamics of which are determined by the properties of the rough energy landscape. In particular, significant roughness slows the motion over the landscape[89] and causes a non-Arrhenius temperature dependence of the time scale of force-induced unfolding.[95,96] Thus, performing force spectroscopy measurements at different temperatures allows one to quantify the energy landscape roughness.

So far, this approach has been used only in a few studies.[97] Results on filamin could be interpreted as arising from an energy landscape roughness of 4 k_BT,[98] whereas that of bacteriorhodopsin transmembrane helices was reported to be 4-6 k_BT.[99] In a similar approach, the roughness of the energy landscape of bimolecular protein complexes along their unbinding reaction coordinate has been found to be slightly larger, of the order of 3-8 k_BT.[100]

This experimental approach provides access to regions of the energy landscape far from those accessed in equilibrium experiments. However, the energy landscape is modified by application of the external force, which may also affect the roughness. Moreover, the quantitative analysis is based on the theory of diffusion in a one-dimensional rough potential,[89] with the protein extension in the direction of the external force taken as the relevant reaction coordinate. Although this approach is valid if relaxation of all other coordinates is fast compared to changes of the reaction coordinate, it may not be fully justified here, given the wide range of coordinates defining the multidimensional energy landscape which may alter the roughness along the particular reaction coordinate chosen.[22,29,30] Thus, *a priori* it is not quite clear how motion in the other dimensions of the multidimensional energy landscape affects the analysis,[89,96] *e.g.* by providing alternative unfolding pathways. Finally, the analysis assumes that the underlying energy landscape, including its roughness, does not change with temperature, which may not be well justified, considering the importance of hydrogen bonding and the hydrophobic effect for protein folding.[98] In particular, there is experimental evidence suggesting an increase of energy landscape roughness with increasing temperature, which has been ascribed to the temperature dependence of the hydrophobic effect.[23-27] Consequently, an alternative interpretation of the experimentally observed temperature dependent force spectroscopy data, namely temperature softening of the protein, is preferred by some authors working in the field.[98]

In a different single-molecule AFM approach, Brujić *et al.* ascribed the experimentally observed distribution of force-induced unfolding times of ubiquitin to an exponential distribution of the unfolding barrier with a width of 5-10 k_BT.[101] They suggested this distribution of the unfolding barrier to arise from different protein conformations, thus yielding a measure of the energy landscape roughness.

Backbone Dynamics Investigated by Geminate Recombination of Disulfide Bonds

Principle of the Method

A different method for investigating polypeptide backbone dynamics was described a few years ago, namely the geminate recombination of a photolyzed aromatic disulfide bond which initially holds the polypeptide in a non-native conformation.[102,103] This method was originally applied to helical model peptides and unusual geminate recombination dynamics were observed which showed that polypeptide backbone segments do not undergo free three-dimensional diffusion as assumed in most previous studies. However, although the authors of these original studies realized that their results contained important information on the conformational dynamics of the polypeptide backbone, no

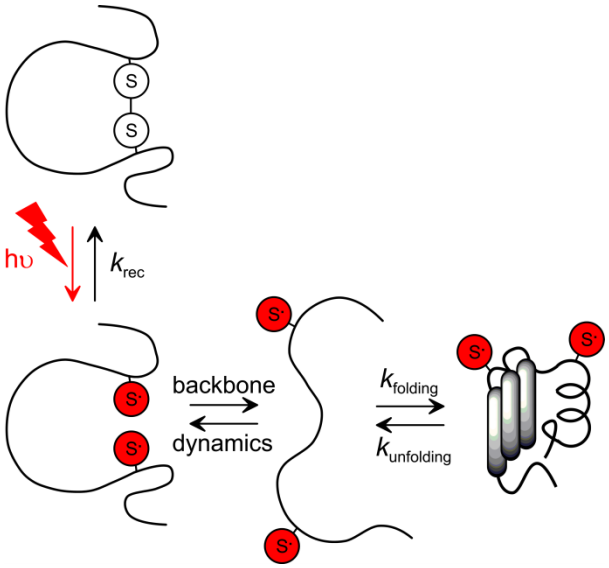

Fig. 3 Principle of the geminate disulfide recombination method for observing backbone dynamics. The peptide or protein is held in a non-native cyclic conformation by an aromatic disulfide bond which can be photolyzed by a short laser pulse (hv), resulting in the formation of thiyl radicals (shown in red) which can be detected by their strong absorbance near 500 nm. Following photolysis, the backbone begins to relax towards its equilibrium conformation, *e.g.* the folded structure under folding conditions, as shown here. Upon contact formation, the radicals can recombine with rate constant k_{rec}, which restores a constrained conformation, or separate again. Since separation and re-encounter of the radicals is governed by the motion of the backbone to which they are tethered, the dynamics of this geminate recombination give access to the backbone dynamics.

detailed interpretation or conclusions were reported. More recently, the method was applied to a small protein and, surprisingly, the same unusual geminate recombination dynamics were found in this case,[32] indicating that the results reflect general properties of the protein backbone. Moreover, the authors of the later report were able to show that the observations result from anomalous subdiffusive motion of backbone segments and provide quantitative information on the energy landscape roughness.

Fig. 3 shows the principle of the method: A peptide or protein is constrained to a non-native conformation by an aromatic disulfide bond between two residues which are far apart in the native structure. This bond can be photolyzed on the picosecond time scale using a UV-laser flash, which triggers the polypeptide backbone's relaxation towards its equilibrium conformation, *i.e.* the native structure under folding conditions or the large conformational space occupied by the denatured protein under unfolding conditions. However, the thiyl radicals created upon bond photolysis are highly reactive, and can geminately recombine when they come back into contact. Initially, they are close to each other and therefore have a high probability of re-encounters and recombination, but over time they are increasingly separated, so that the rate of geminate recombination of the surviving radicals decreases with time. Since motion of the radicals is slaved to the motion of the backbone to which they are tethered, these re-encounter and recombination dynamics are governed by the motion of the backbone. Therefore, the observation of the radicals' recombination dynamics provides an alternative experimental method for observing backbone

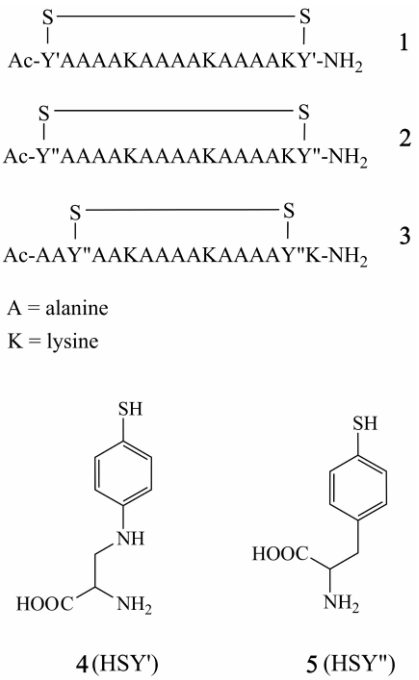

Scheme 1 Model peptides with aromatic disulfide bond crosslink dynamics.

The disulfide recombination method is highly complementary to the equilibrium methods described above. It allows the observation of backbone motions far from equilibrium, if the initial constrained conformation is non-native, and thus gives access to high-lying regions of the energy landscape, unlike the equilibrium loop formation experiments described above, which are limited to conformations with an energy of at most a few k_BT. Furthermore, there is no intrinsic limit to the time scale accessible by the disulfide recombination method. Unfortunately, non-aromatic thiyl radicals have intrinsically slow recombination dynamics,[104] so that they cannot be used in this method. However, synthesis protocols for the incorporation of aromatic disulfides into custom-synthesised peptides[105] or proteins[106] are available.

Results

The disulfide recombination method for observing backbone dynamics was first applied to the α-helical model peptides **1**-**3** shown in Scheme 1,[102,103] which were synthesised by standard methods using the modified amino acids **4** and **5**.[105] CD spectroscopy confirmed that before oxidation of the thiol groups to form the disulfide bond these peptides have significant helicity,[105] as expected from their high alanine content. Formation of the disulfide bond leads to a significant reduction of the helical content, verifying that the disulfide cross-link forces the peptides to adopt non-native backbone conformations.

Photolysis of peptides **1** - **3** with short UV laser flashes induces the ultrafast formation of transient absorbance with spectral maxima at 620 nm and 500 nm for peptide **1** (Fig. 4) and peptides **2** and **3**, respectively. These wavelengths are characteristic for the respective thiyl radical absorbance,[107-110] reflecting the different chemical nature of the thiol groups in the modified amino acids **4** and **5**, with significant charge transfer expected to occur from the sulfur radical to the *para*-amino group in **4**. Formation of this

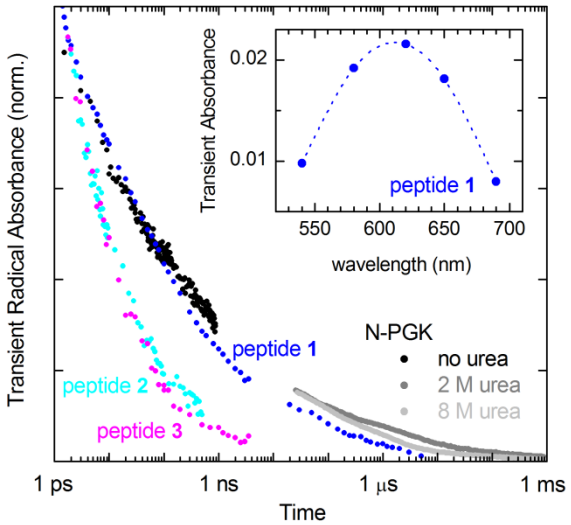

Fig. 4 Time dependence of the transient thiyl radical absorbance observed after photolysis of the aromatic disulfide bond in peptide **1** (blue, measured at 620 nm),[102] peptide **2** (cyan, 500 nm),[102] peptide **3** (magenta, 500 nm)[103] and N-PGK[32] in the absence of urea (black, 560 nm, ps- to ns-time scale), in 2 M urea (dark grey, 488 nm, ns- to ms-time scale) and 8 M urea (light grey, 488 nm, ns- to ms-time scale) , normalized to the value at short times. The inset shows the transient absorbance spectrum of peptide **1** at a time of 100 ps after photolysis.[102]

transient absorbance confirms that ultrafast disulfide bond breaking occurs upon UV flash photolysis, as had been observed previously for model disulfide compounds.[105,109-111] The transient absorbance disappears over a wide range of time scales (1 ps – 10 µs) due to geminate recombination of the disulfide bonds (Fig. 4). The side chain amino group of **4**, which is in *para*-position to the thiol, significantly reduces the reactivity of the thiyl radical and thus yields slower geminate recombination in peptide **1** compared to **2** and **3**. This mirrors results found for model disulfides and was ascribed to the formation of an intramolecular charge transfer complex between the amino group and the thiyl radical.[107,109,112]

More recently, Milanesi *et al.* developed a method for trapping proteins in non-native conformations using compound **6** (Scheme 2), which consists of an aromatic disulfide flanked by two maleimide groups.[106] Under unfolding conditions, this compound can be used to link two cysteines which are remote in the native structure, thus preventing the protein from adopting its native conformation and constraining it to a non-native conformation even upon return to folding conditions, see Scheme 2. This strategy was used to incorporate an aromatic disulfide into the N-terminal domain of phosphorglycerate kinase from *Geobacillus steareothermophylus* (N-PGK, 174 amino acids).[106] CD-, NMR- and fluorescence spectroscopy were used to show that at low denaturant concentrations the crosslinked protein adopts a molten-globule like non-native conformation with significantly reduced tertiary structure, albeit almost native secondary structural content.[32,106] Chemical reduction of the crosslink restores the native behaviour, suggesting that UV photolysis of the crosslink also should trigger relaxation towards the native structure.

Transient absorbance measurements[32] confirmed fast disulfide bond photolysis in cross-linked N-PGK by short UV laser flashes, as shown by the appearance of the typical thiyl radical absorbance in the region 500-600 nm found in helical peptides **1** – **3** and model compounds.[102,107-110] In this case, recombination of the radicals could be followed over an even wider range of time scales, covering nine orders of magnitude, from 1 ps to 1 ms, Fig. 4.

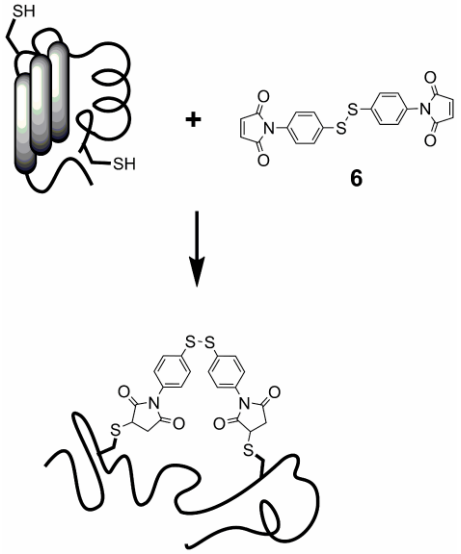

Scheme 2 Principle of cross-linking of a protein with an aromatic disulfide[106]

The wide range of time scales over which geminate recombination[‡] is observed in these experiments is partly due to the increasing separation of the radicals. They are generated in close vicinity of each other by the photolysis reaction, but then get separated due to motion of the backbone towards the equilibrium conformation. This reduces the chances of a re-encounter which is a necessary pre-requisite for recombination, and hence the probability of recombination of the surviving radicals decreases with time. A useful quantitative measure of the time-dependent probability for a re-encounter and recombination of a surviving radical pair is the instantaneous rate constant for recombination, $k_{inst}(t)$, which is given by[††]

$$k_{\mathrm{inst}}(t) = -\frac{\mathrm{d}c(t)/\mathrm{d}t}{c(t)} = -\frac{\mathrm{d}A(t)/\mathrm{d}t}{A(t)} \qquad (1),$$

where t is the time after photolysis and $c(t)$ is the surviving radical concentration, which is directly reflected in the measured transient absorbance $A(t)$.

Fig. 5 shows the time dependence of $k_{inst}(t)$ for the helical model peptides and N-PGK, calculated from the transient absorbance results given in Fig. 4. It can be seen that these results show a highly unusual power law, $k_{inst}(t) \sim t^{-0.94(\pm 0.03)}$, over the whole time window. This is found for the simple helical model peptide **1** which lacks tertiary structure as well as the protein N-PGK which in its native state has well-defined secondary and tertiary structure. The results for peptides **2** and **3** have higher uncertainty because of the faster recombination and hence smaller transient absorbance, but are compatible with the same power law $k_{inst}(t) \sim t^{-0.94}$. Moreover, the same power law is even found in the absence of significant secondary or tertiary structure (N-PGK at 8 M urea). This universality of the power-law time dependence of $k_{inst}(t)$, which holds over nine orders of magnitude in time and is independent of the primary sequence or secondary or tertiary

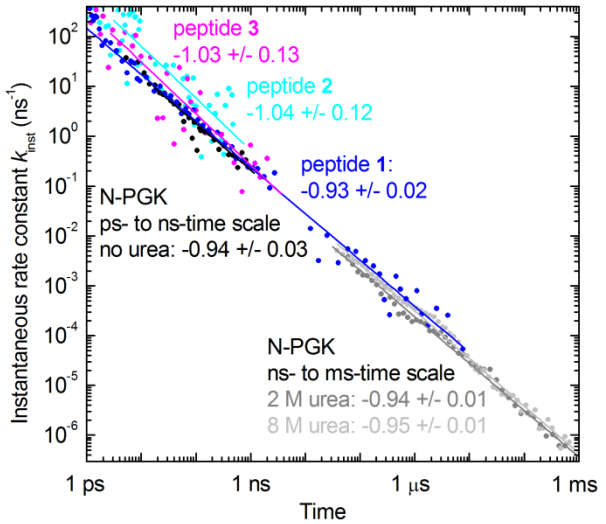

Fig. 5 Time dependence of the instantaneous rate constant for recombination, $k_{inst}(t)$, for peptide **1** (blue),[102] peptide **2** (cyan),[102] peptide **3** (magenta)[103] and N-PGK[32] in the absence of urea (black, ps- to ns-time scale), in 2 M urea (dark grey, ns- to ms-time scale) and 8 M urea (light grey, ns- to ms-time scale). Solid lines are the results of power law fits; also given are the fit results. Experiments were restricted to a shorter time scale and less data (resulting in lower signal-to-noise) were collected for peptides **2** and **3** because of the fast recombination found in these peptides, so that power law fits to these data yielded less reliable results.

structure is most intriguing, since it points towards an intrinsic property of the polypeptide backbone. Notably, it was observed not only experimentally, but was also confirmed in MD simulations.[113]

Theory of Diffusion-Controlled Geminate Recombination

Extensive numerical simulations were undertaken in an attempt to identify the origin of the experimentally observed unusual power law behaviour of the instantaneous rate constant, $k_{inst}(t)$.[32] As described in detail in the following section, it was shown that the observed power law time dependence of $k_{inst}(t)$ is not compatible with normal three-dimensional diffusion of the radicals. This is true even when accounting for the well-characterised properties of the polypeptide backbone to which they are bound, such as tethering, excluded volume or chain stiffness, all of which affect the available conformational space and hence the equilibrium radical-radical distance distribution. Thus, polypeptide backbone segments do not move by normal diffusion, which often has been assumed in the analysis of similar experiments, such as the loop formation experiments described above. On the other hand, a wide distribution of trapping times can be shown to yield the observed recombination dynamics, but also leads to so-called subdiffusional motion and it was concluded that the relative motion of polypeptide backbone segments is strongly subdiffusive. This behaviour is a consequence of the roughness of the conformational energy landscape and the experimental results presented above allow quantification of this roughness.

Normal Diffusion

The term "normal diffusion" is used to describe diffusional motion which in the absence of any constraints ("free" diffusion) is described by the "normal" Fick's law diffusion equation

$$\frac{\partial}{\partial t} p(\boldsymbol{x},t) = D\nabla^2 p(\boldsymbol{x},t) \qquad (2),$$

where $p(\boldsymbol{x},t)$ is the probability density of finding a particle at position $\boldsymbol{x}$ at time t, D the diffusion coefficient and ∇ the Nabla (differential) operator. This equation results in a linear increase of the mean square displacement of a diffusing particle with time,[‡‡] $\langle r^2(t)\rangle \propto t$.

Geminate recombination of radicals which initially are in close contact and undergo geminate recombination controlled by normal diffusion has been widely investigated, both theoretically[114] and experimentally.[111,115] The time-dependent survival probability, $P(t)$, of such radicals is affected by the initial pair separation, r_0, at which the radicals are generated, their relative diffusion constant, D, the contact distance, σ, at which recombination occurs, and a second-order rate coefficient, k_{rec}, which describes the probability of recombination at σ. $P(t)$ can be expressed in analytical closed form:[114]

$$P(t) = 1 - \frac{\lambda}{\kappa(1+\lambda)}\left\{\operatorname{erfc}\left[\frac{\kappa-1}{2\sqrt{t/\tau_0}}\right] - e^{(1+\lambda)(\kappa-1)} \times e^{(1+\lambda)^2(t/\tau_0)}\operatorname{erfc}\left[(1+\lambda)\sqrt{t/\tau_0} + \frac{\kappa-1}{2\sqrt{t/\tau_0}}\right]\right\} \qquad (3)$$

Here, $\kappa = r_0/\sigma$, $\lambda = k_{rec}/k_D$, $k_D = 4\pi\sigma D$, and $\tau_0 = \sigma^2/D$; erfc(x) is the complementary error function. This theoretical prediction has been shown experimentally to be valid for the geminate recombination of aromatic thiyl radicals in solution.[111,115]

The instantaneous rate constant $k_{inst}(t) = -(dP(t)/dt)/P(t)$ can be easily calculated from this expression. Fig. 6 (black lines) shows the time dependence of $P(t)$ and $k_{inst}(t)$ for typical values of r_0, σ and k_{rec} taken from experimental results for aromatic disulfides[111,115] and a value of the diffusion constant D which is typical of those found for polypeptide backbone segments in loop formation experiments, see above. It can be seen that $k_{inst}(t)$ switches from an initial power law $k_{inst}(t) \sim t^{-0.5}$ to $k_{inst}(t) \sim t^{-1.5}$; this switch occurs on the ns-time scale, corresponding to diffusion over a length scale given by σ. This time dependence results from the fact that initially only diffusion of the radicals in one dimension (away from each other) is of significance, whereas after sufficient separation diffusion in all three dimensions becomes relevant. It should be noted that this behaviour is independent of the exact parameters chosen, which were varied over a wide range without affecting these power laws and the fact that switching occurs within a few orders of magnitude in time.[32] Thus, the assumption of simple free three-dimensional diffusion of the radicals is not compatible with the observed power law $k_{inst}(t) \sim t^{-0.94}$ over nine orders of magnitude in time. Clearly, the properties of the polypeptide backbone to which the radicals are bound affect their diffusion beyond slowing them down, which was accounted for by taking the value of D of backbone segments.

The most obvious effect of the polypeptide backbone on the radical diffusional dynamics is its tethering effect which prevents the radicals to escape from each other. This effect is usually

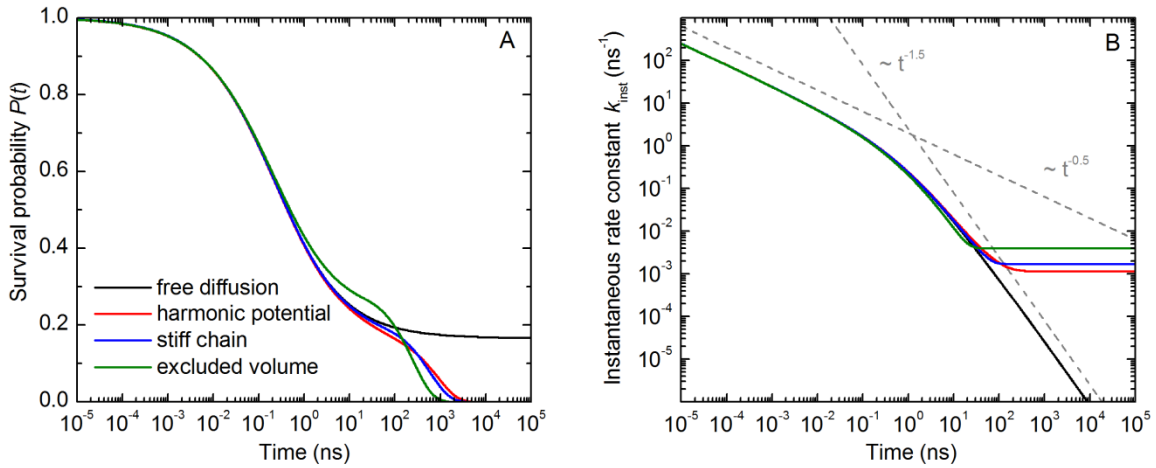

Fig. 6 Simulation of geminate recombination of thiyl radicals assuming normal diffusion: (A) time dependence of the survival probability $P(t)$; (B) time dependence of the instantaneous rate constant of recombination $k_{inst}(t)$, calculated from $P(t)$. Black lines assume freely diffusing radicals and are based on Eq. (3); the other lines are the results of finite element simulations for diffusion in a harmonic potential (red) or in potentials accounting for the effects of backbone chain stiffness[40] (blue) or excluded volume[49] (green). Parameters: $r_0 = \sigma = 7.2$ Å, $k_{rec} = 1.1\ 10^{12}$ cm^{3}mol^{-1}s^{-1}, $D = 4$ Å^2/ns; $L = 45$ Å (harmonic potential); $l_p = 12$ Å (stiff chain); $d_\alpha = 5.5$ Å (excluded volume).

included by assuming relative motion in a harmonic potential which correctly describes the Gaussian end-to-end (or residue-to-residue) distance distribution expected for a random coil tether.[57,116] For N-PGK and peptides 1-3, the parameters of this harmonic potential are chosen to yield an equilibrium root mean square distance, L, of the radicals on the order of 35-45 Å, as expected for radicals separated by 11 and 17 amino acid residues, respectively.[32] Geminate recombination of radicals diffusing in such a harmonic potential was studied using finite-element simulations,[32] since no closed analytical solution is available for this problem. Fig. 6 (red lines) shows the results of such simulations for the same reaction and diffusion parameters as used above, but including a harmonic potential corresponding to L = 45 Å. For short times, these simulations yield exactly the same results for $P(t)$ and $k_{inst}(t)$ as simulations assuming fully free diffusion, since the harmonic potential allows for virtually free diffusion at short radical distances, when the tether is not stretched. Only after diffusion over a length scale comparable to L, when the surviving radicals begin to approach their maximum separation, do the results deviate. Unlike freely diffusing radicals, which can escape from each other to infinite distances, tethered radicals recombine with a yield of 100%. Furthermore, the instantaneous rate constant for recombination adopts a time-independent value after conformational equilibration on the time scale of 10-100 ns, which corresponds to diffusion over L, in agreement with the loop formation results discussed above. Thus, inclusion of the tethering effect yields an even larger disagreement between the experimentally observed and the simulated time dependence of $k_{inst}(t)$, indicating that other properties intrinsic to the polypeptide backbone are the cause of the unusual recombination dynamics observed here. Again, these general conclusions were verified for a wide range of parameters.[32]

The simulations assuming a harmonic potential only account for the tethering effect of the polypeptide backbone linking the two radicals but do not take into consideration other important properties of the backbone, such as chain stiffness and excluded volume effects. Chain stiffness is caused by the finite bending rigidity of the backbone and causes a preferential propagation of the backbone in the direction of the initial section over a number of residues. The correlation length of the backbone propagation direction is referred to as the persistence length, l_p, for which values in the range from 2 to 15 Å have been reported for polypeptides.[40,117] Excluded volume, on the other hand, refers to the trivial fact that a residue cannot occupy the volume already occupied by another and can be quantified by a hard-sphere diameter, d_α, which has a value of a few Å. Both of these effects reduce the number of conformations where two residues are in close contact, and thus modify the Gaussian distribution of residue-to-residue distances which is expected for a truly random coil polymer linker; several such modified distributions have been suggested in the literature based on experimental results or theoretical considerations.[40,49,55,118] All of these distributions include terms accounting for the tethering effect. For investigating the effect of chain stiffness and excluded volume on the geminate recombination of thiyl radicals, extensive numerical simulations were undertaken where the harmonic potential was replaced by modified potentials corresponding to the distributions expected from these effects.[32] Fig. 6 shows two examples, using the potential suggested by Lapidus *et al.*[40] accounting for chain stiffness with a persistence length, l_p, of 12 Å (blue line), and that suggested by Buscaglia *et al.*[49] accounting for excluded volume with a hard-sphere diameter, d_α, of 5.5 Å (green line), respectively. Although inclusion of these effects modifies the motion of the radicals and hence their geminate recombination dynamics, the effects are only of a minor nature. The initial time dependence of $P(t)$ and $k_{inst}(t)$ is identical to that observed for free diffusion or diffusion in a harmonic potential. Deviations are only observed after times corresponding to diffusion over the relevant length scales of the effects, l_p and d_α, respectively. However, even then the general behaviour of the instantaneous rate constant $k_{inst}(t)$ is not changed – it switches from an initial power law $k_{inst}(t) \sim t^{-0.5}$ to $k_{inst}(t) \sim t^{-1.5}$ on the ns-time scale and then becomes independent of time on the time scale of 10-100 ns.

Thus, also the inclusion of chain stiffness and excluded volume does not resolve the discrepancy between the experimentally observed power law $k_{inst}(t) \sim t^{-0.94}$ over nine orders of magnitude in time and the simulations assuming normal diffusion. Again, these general conclusions were verified for a wide range of parameters.[32]

Thus, it was concluded that normal diffusional behaviour of polypeptide segments, which is characterised by a linear increase of the mean square displacement, $\langle r^2(t) \rangle \propto t$ in the absence of other constraints, cannot account for the experimental results reported above, even if expected effects of the polypeptide backbone, such as tethering, excluded volume and chain stiffness, are taken into account.

Subdiffusion

Anomalous diffusion is characterised by a nonlinear time dependence of the mean square displacement,[§§] $\langle r^2(t) \rangle \propto t^{\alpha}$. Recently, such behaviour has been observed experimentally, for example for biomolecules inside cells or in membranes[119] or for the motion of sticky particles on a surface.[120] Typically, the anomalous diffusion parameter α has a value of less than 1, and the motion then is referred to as "subdiffusion". Intraprotein subdiffusional motion has been found, both for local motions on the pico- to nanosecond time scale[121,122] and for larger conformational changes on the millisecond to second timescale.[123,124] Subdiffusional motion can be caused by a variety of effects, such as crowding,[119] the presence of randomly distributed inhomogeneous traps with a wide distribution of trapping times,[120,125-127] or – in the case of polymer segments – the chain connectivity of the polymer backbone, i.e. the fact that a polymer segment cannot move independently of the other segments even if no direct interaction between non-neighbouring residues is taken into account..[128-133]

The last effect has been studied widely using the Rouse or Zimm models which simulate the dynamic behaviour of a polymer using beads connected by harmonic springs.[134]. It was shown theoretically and by numerical simulations that for the simple "free-draining" Rouse model, which ignores any hydrodynamic effects, the mean square displacement increases as $\langle r^2(t) \rangle \propto t^{0.5}$, or $t^{0.54}$ if self-avoidance of the chain is included.[128-131] The somewhat more realistic "nondraining" Zimm model accounts for solvent-induced hydrodynamic interactions between the segments and yields $\langle r^2(t) \rangle \propto t^{0.67}$.[135] Segments of single- and double-stranded DNA have been shown to follow such subdiffusive motion over several orders of magnitude in time.[135,136]

This subdiffusive behaviour in the Rouse or Zimm models is predicted to occur only over the limited time interval between the shortest and the longest Rouse relaxation times.[137] In the Supporting Information, we present explicit results which show that the finite Rouse model[132,138,139] predicts subdiffusive behaviour, $\langle r^2(t) \rangle \propto t^{0.5}$, but this behaviour extends over not more than two orders of magnitude in time for peptides **1** – **3** and not more than at most four orders of magnitude for N-PGK (130 ps - 15 ns for peptides **1** – **3** and 120 ps – 1.5 μs for N-PGK). At shorter times, residue diffusion is expected to follow normal diffusion, whereas at longer times full equilibration between all conformations has taken place, so that the mean square displacement of residues with respect to each other does not change any further. The inclusion of internal friction, which recently has been highlighted to be of significant importance for the dynamics of unfolded polypeptides, see above, significantly reduces the width of the relaxation time spectrum of the Rouse model, particularly for relatively short polymers, such as the ones discussed here.[86,140] Although to the best of our knowledge, the subdiffusive behaviour of a Rouse chain in the presence of internal friction has not been investigated explicitly, the narrowed relaxation time spectrum is expected to lead to a correspondingly narrower time interval over which subdiffusive behaviour is expected. Moreover, the N-PGK residues to which the thiyl radicals are tethered are separated by only 11 residues, so that their relative diffusion is expected to lead to equilibration on a significantly shorter time scale than that estimated from the Rouse relaxation time of the whole polypeptide.[86,141] Thus, it is not expected that the subdiffusive behaviour of a polypeptide backbone arising from its chain connectivity could be the main cause of the experimentally observed unusual power law, $k_{inst}(t) \sim t^{-0.94}$, which extends over much wider time scales.

On the other hand, subdiffusive intraprotein backbone diffusion can also be caused by other effects, such as inhomogeneous trapping due to the multitude of local interactions which give rise to the rugged potential energy landscape with its hierarchy of well depths,[123,142,143] as shown schematically in Fig. 1B. The time-dependent survival probability, $P(t)$, of geminately recombining radicals which undergo subdiffusive motion because of a wide range of local trapping times can be given in analytical form.[144] The underlying theoretical treatment assumes particles undergoing a random walk with a fixed jump size, but an exponential distribution of jump activation energies E_j, $g(E_j) \sim \exp(-\alpha E_j/k_BT)$, which results in a wide distribution of jump times if α is small. It should be noted that in the context of backbone segment diffusion, the jump activation energies E_j correspond to the depths of the local wells on the rough energy landscape which temporarily trap the backbone in particular conformations (Fig. 1). It can be shown that this random walk leads to subdiffusive behaviour with $\langle r^2(t) \rangle \propto t^{\alpha}$. Notably, for $\alpha = 1$, the distribution of jump activation energies has a width corresponding to k_BT, so that the distribution of trapping times is narrow and normal diffusional behaviour is recovered. For simulating geminate recombination dynamics under subdiffusive conditions, radicals are assumed to recombine with a certain probability whenever they come into contact at contact distance σ.

This theoretical treatment was used to simulate the time dependence of $P(t)$ and $k_{inst}(t)$ under subdiffusive conditions,[32] analogous to the simulations for normal diffusion described in the previous section. Fig. 7 shows typical results, using the same parameters as used for the free normal diffusion simulations in Fig. 6, but varying the subdiffusional parameter α between 1, corresponding to normal diffusion, and 0.1, which simulates strongly subdiffusive behaviour with a width of the jump activation energy distribution of 10 k_BT. As expected, for $\alpha = 1$ these simulations predict the same time dependence of geminate recombination as simulations assuming normal diffusion (dashed blue lines in Fig. 7), with the instantaneous rate constant $k_{inst}(t)$ decaying $\sim t^{-0.5}$ at short times and $\sim t^{-1.5}$ at long times. For lower values of α, these two phases of the time dependence of $k_{inst}(t)$ still can be approximated by power laws, but the power for the

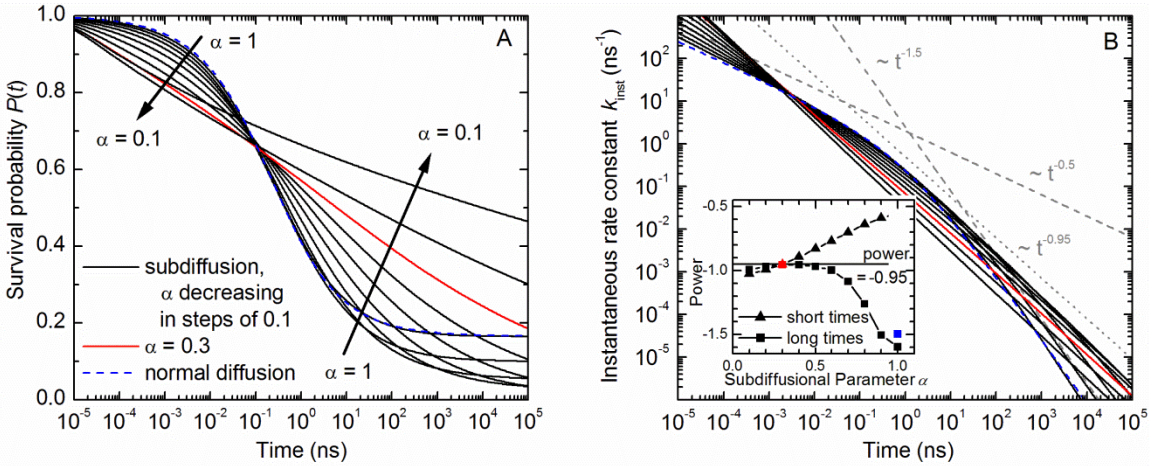

Fig. 7 Simulation of geminate recombination of thiyl radicals assuming subdiffusion: (A) time dependence of the survival probability $P(t)$; (B) time dependence of the instantaneous rate constant of recombination $k_{inst}(t)$, calculated from $P(t)$. Also included are the results for normal free diffusion (dashed blue lines). The inset in (B) shows the power of the $k_{inst}(t)$ time dependence, obtained from power law fits for short and long times, respectively, against the subdiffusional parameter α. Highlighted in red are the results for a value of 0.3 for α. Parameters: $r_0 = \sigma = 7.2$ Å, $k_{rec} = 1.1\ 10^{12}$ cm^{3}mol^{-1}s^{-1}, $D = 4$ Å^2/ns.

fast phase decreases from -0.5 to -1, whereas that for the slow phase increases from -1.5 to -0.95 for $\alpha = 0.3$ and then decreases again slightly. Most interestingly, for $\alpha = 0.3$, the two phases become essentially indistinguishable and the simulations predict $k_{inst}(t) \sim t^{-0.95}$ for the whole time window over which the simulations were performed, encompassing ten orders of magnitude in time. Similar results were found for a wide range of parameters.[32]

Thus, the experimentally observed power law time dependence $k_{inst}(t) \sim t^{-0.94}$ over nine orders of magnitude in time can be reproduced almost perfectly with simulations assuming a wide range of local trapping times which leads to subdiffusive motion of the peptide segments to which the radicals are bound, whereas normal diffusion is not able to reproduce this power dependence even when accounting for the tethering, chain stiffness and excluded volume effects of the polypeptide backbone. This provides compelling evidence that the relative motion of polypeptide backbone segments is strongly subdiffusive, with a subdiffusional parameter α of around 0.3.

It should be noted that these simulations assume free diffusion of the radicals, *i.e.* diffusion in the absence of chain connectivity or any effects caused by the backbone other than trapping in local conformations on the rugged energy landscape. As described above, chain connectivity may lead to subdiffusive behaviour, but only over a limited range of times. Chain stiffness and excluded volume effects can be simulated by the introduction of suitable interaction potentials, but these potentials have no major effect on the overall recombination dynamics for normal diffusion; it is assumed here that the same is true for subdiffusive motion. Similarly, tethering does not affect radical recombination under normal diffusion control at short times, but it leads to a time-independent value of $k_{inst}(t)$ after conformational equilibration, see Fig. 6. The same effect is expected for the case of *subdiffusively* moving radicals which are tethered by a polypeptide. However, whereas for normal diffusion the time scale of equilibration is directly determined by the size of accessible space (*i.e.*, the length of the tether) and the effective diffusion constant, for subdiffusion caused by a wide range of trapping times, an additional parameter becomes important, namely the longest trapping time.¶ Full equilibration only can occur on time scales exceeding this longest trapping time. It also should be noted that a subdiffusively moving particle spends a larger fraction of time close to its initial position than a particle undergoing normal diffusion, which leads to significantly slower equilibration over the accessible space.[126,145] In the Supporting Information, we present the results of random-walk simulations which confirm that normal diffusion over the length of the tether (35-45 Å) occurs on the 10-100 ns time scale when assuming a diffusion constant as determined from the equilibrium loop formation experiments described above. In contrast, subdiffusive motion in the presence of a wide distribution of trapping times leads to much slower motion of the polypeptide segments; a separation of the radicals by only a few Å is predicted even after 1 ms for strongly subdiffusive motion ($\alpha = 0.3$), see Fig. S2. Thus, it is not surprising that no such equilibration is observed in the experimental data of Fig. 5, which extend only to the millisecond time scale.

Subdiffusive Protein Backbone Motion

Comparison of the data shown in Fig. 5 with the simulations described in the preceding section shows that the diffusive motion of a polypeptide backbone cannot be described by the normal diffusion equation, Eq. (2). On the other hand, the assumption of strongly subdiffusive behaviour arising from a wide range of local trapping times yields perfect agreement of the simulation results with experimental data over the full time range of the experiments. The experimental results include data from helical model peptides as well as a real protein, so that it can be concluded that subdiffusive behaviour is an inherent property of a polypeptide, independent of primary sequence or secondary and tertiary structure. Furthermore, it was observed to pertain over a wide range of time scales, encompassing at least nine orders of magnitude in time, from picoseconds to milliseconds, for the protein investigated here.

On first sight, the results of the geminate disulfide recombination experiments appear to be in conflict with the results of the equilibrium loop formation experiments described above. Most of the publications in this field report single exponential dynamics for loop formation in unstructured peptides or denatured proteins on the nano- to microsecond time scale; this is often taken as evidence that complete conformational equilibration occurs on this time scale by normal diffusion of backbone sections, since theoretical considerations predict close-to-single exponential loop formation dynamics under this condition.[57] Such diffusional equilibration also predicts a time-independent instantaneous rate constant for geminate recombination, $k_{inst}(t)$, after diffusion over the length of the peptide chain has occurred, Fig. 6. In contrast, the experimental results shown in Fig. 5 clearly show $k_{inst}(t)$ decreasing with time on the time scale of several microseconds in the helical model peptide, or the 1 ms-time scale in the denatured protein, indicating that full equilibration has not been achieved yet.

This apparent contradiction suggests that the observation of single exponential loop formation dynamics may not be a sensitive indicator for full conformational equilibration taking place on the experimental time scale. To the best of our knowledge, no theory of polymer loop formation dynamics from an equilibrium conformational distribution exists for subdiffusive conditions. However, particle diffusion in the presence of a distribution of traps only shows anomalous behaviour if a random initial distribution of starting sites is assumed, whereas an equilibrium initial distribution, where the particle is more likely to start in a site corresponding to a deep trap, yields normal diffusion, *i.e.* $<r^2(t)> \propto t$.[120,146,147] This indicates that equilibrium initial conditions partly cancel the effect of subdiffusive motion or the underlying hierarchy of traps, which might explain the close-to-single exponential dynamics observed in equilibrium loop formation experiments even if full equilibration is not achieved on the experimental time scale. Similarly, MD simulations of peptide loop formation, which do reproduce the experimental power law $k_{inst} \sim t^{-0.94}$ if the ends initially are in close proximity, yield almost exponential dynamics for equilibrium initial conditions.[113] In this context, it is also important to bear in mind that the time scales accessible in the equilibrium loop formation experiments are limited by the intrinsic lifetime of the reporter state or single molecule diffusion dynamics. Finally, deviations from exponential dynamics on time scales of 100 ns or slower have in fact been reported in many of the loop formation experiments.[13,15-17,20,22,37,43,44,49,50,52,55,62,75-80,82,85,148] These can often be ascribed to experimental artefacts inherent in the method, such as contributions from photoproducts other than the reporter state, or to sample heterogeneity, impurities or intermolecular effects. However, these additional dynamic components further limit the conclusions that can be drawn on complete conformational equilibration of polypeptides on the nano- to microsecond time scale. Thus, it seems highly likely that the limitations of the equilibrium loop formation methods may prevent the observation of the slower time scales of conformational equilibration which are shown by the results in Fig. 5, and therefore also hide the need of considering anomalous diffusion explicitly. On the other hand, comparison of loop formation dynamics obtained with different probes has been suggested to show time- and length-scale dependent intrapeptide diffusion,[20,149] an effect which is identical to subdiffusion. It should also be noted that, in spite of these potential problems, the numerous results and conclusions obtained from the loop formation experiments have contributed significantly to our understanding of polypeptide backbone dynamics.

Intraprotein subdiffusional motion has been experimentally observed before. Neutron scattering data indicated strongly subdiffusive motion of protein atoms and water molecules in the protein hydration layer on the picosecond time scale.[121] MD simulations yielded evidence for subdiffusive dynamics of backbone and side chain dihedral angles on the pico- to nanosecond time scale.[122] MD simulations also showed subdiffusive behaviour of the distance fluctuations between electron donor and acceptor groups in a protein on the picosecond time scale.[142] On the same protein, single molecule fluorescence experiments confirmed the relative donor-acceptor motion to be subdiffusive on the millisecond to second timescale.[123,124] Most interestingly, the subdiffusive parameter α found in these experiments has a value of 0.31,[123] which is in good agreement with the value required to simulate the data in Fig. 5. All of these observations were obtained on proteins in equilibrium and thus related to small scale fluctuations. The experimental data obtained using geminate recombination of a disulfide bond, Fig. 5, yield the same conclusion of subdiffusive motion of the polypeptide backbone, but pertain to the full time scale from pico- to milliseconds, and thus span the time gap between the previous results. Moreover, they relate to peptides and proteins which are not in equilibrium and are undergoing large scale conformational changes.

As discussed above and in more detail in the Supporting Information, intraprotein subdiffusional motion has been suggested by theoretical polymer models. The simple Rouse model predicts the mean square displacement of polymer segments to follow $<r^2(t)> \propto t^{0.5}$, although this behaviour extends only over a limited time range - two orders of magnitude in time for peptides **1** – **3**, and at most four orders of magnitude in time for N-PGK. Moreover, the simulations shown in Fig. 7 indicate that a subdiffusive parameter of 0.5 is not sufficient to explain the experimentally observed power law $k_{inst}(t) \sim t^{-0.94}$ over nine orders of magnitude in time. The more realistic Zimm model predicts even less subdiffusive behaviour, $<r^2(t)> \propto t^{0.67}$, over an even shorter time range. Thus, whereas chain connectivity may make a small contribution towards the subdiffusive behaviour of the polypeptide backbone, it can be ruled out as the main cause of the observed unusual geminate recombination dynamics. On the other hand, a hierarchy of traps on the conformational landscape which provide a wide distribution of trapping times can be shown to yield strongly subdiffusive behaviour over the ps- to ms-time range and at the same time predicts geminate recombination dynamics which are in excellent agreement with the experimental observations. This conclusion is further supported by the fact that the existence of traps with a wide distribution of depths/trapping times is sufficient to predict $k_{inst}(t) \sim t^{-0.94}$, even in the absence of any diffusional separation of the radicals, as shown by the simple inhomogeneous trap model for geminate recombination which is described in detail in the Supporting Information. In this model, the radicals become trapped in close vicinity of each other

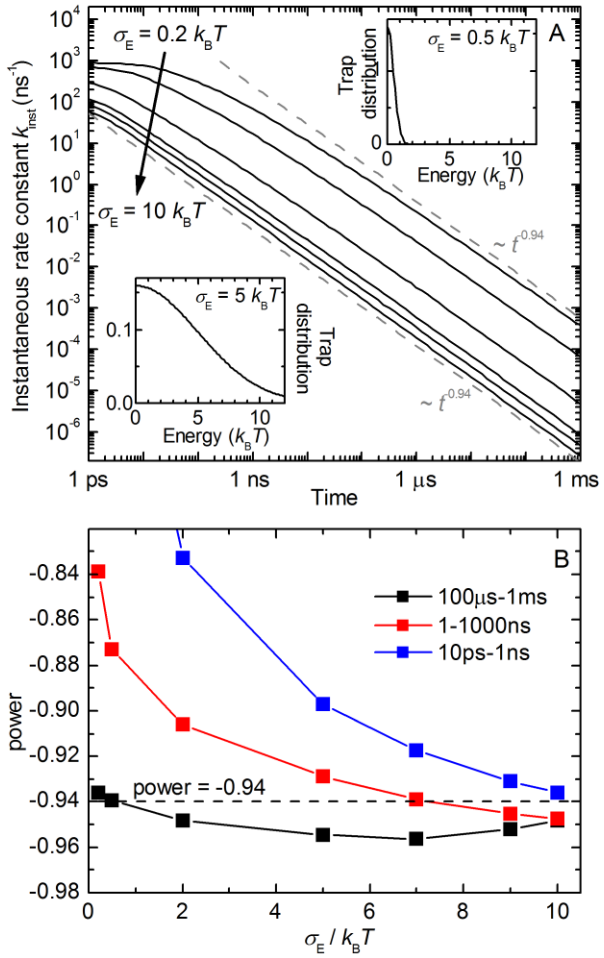

Fig. 8 Results of simulations using the simple trap model for geminate recombination which ignores diffusional motions of the radicals, but assumes a Gaussian distribution of trap depths with variance σ_E^2 (see Supporting Information for details). (A) Time dependence of the instantaneous rate constant of recombination $k_{inst}(t)$, for k_0 = 1 ps^{-1}, E_0 = 0, σ_E/k_BT = 0.2, 0.5, 2, 5, 7, 10. The dotted lines show the power law ~ $t^{-0.94}$. The insets show the distributions for σ_E = 0.5 k_BT and 5 k_BT, respectively. (B) Powers of the time dependence of $k_{inst}(t)$ vs. the width of the trap depth distribution, from power law fits over different time intervals.

immediately after bond photolysis and recombine directly upon escape from this trap. Our calculations show that a trap depth distribution with a width of several k_BT is sufficient to yield $k_{inst}(t) \sim t^{-0.94}$ over a wide time range, see Fig. 8. Thus, the unusual geminate recombination dynamics are not necessarily a direct consequence of subdiffusional motion, but subdiffusion and recombination dynamics seem to both result from the wide distribution of traps on the energy landscape. It is also interesting to note that polypeptides appear to undergo significantly more subdiffusive motion than single- or double-strand DNA, for which good agreement with the Zimm model predictions has been found.[135,136]

The fact that the motion of protein backbone sections is highly subdiffusional is of considerable interest in the context of discussing protein folding mechanisms. Subdiffusive motion, characterised by a non-linear time dependence of the mean-square displacement $\langle r^2(t) \rangle \propto t^{\alpha}$, results in preferential motion through the nearby space, but delays exploration of accessible space which is farther away.[126,145] This suggests that proteins with low contact order, in which many native contacts are formed by residues which are close to each other in the primary sequence, should fold more easily and rapidly than proteins with high contact order. It is intriguing to note that such a correlation between the contact order and folding times has indeed been reported, at least for small proteins.[150] On the other hand, subdiffusive motion makes it less likely that native contacts between residues which are far from each other in the primary sequence are formed as an early step of folding. Formation of such native contacts is much more likely to be preceded by formation of secondary structure or other native contacts which restrict the space accessible to the residues.

The subdiffusive nature of backbone motion will need to be considered in more detail for theoretical investigations of protein folding. Because of the high complexity of proteins, these necessarily make use of some simplifications; for example, thermally driven motion in a one-dimensional idealised potential along some folding coordinate is often used for modelling the folding rate constant using Kramers' theory.[11,27,151] In a simplified approach, energy landscape roughness in these simulations is approximated by increased friction. However, this may not correctly account for all aspects of the subdiffusional backbone motion in three-dimensional real space, such as the efficient search through nearby space and less efficient exploration of larger distances, as well as dynamic effects, such as a dependence of effective friction on the time scale of the motion.[90] More advanced approaches, such as the fractional Fokker-Planck equation[126,127,152] or the generalized Langevin equation with fractional Gaussian noise[90,123,153] which describe subdiffusional motion in a potential, may be required for simulating protein conformational changes.

Energy Landscape Roughness

The experimental results shown in Fig. 5 not only confirm subdiffusional motion of the polypeptide backbone, but together with the simulations in Fig. 7 also provide an alternative method for measuring the roughness of the protein's energy landscape.

Subdiffusion over such a long time scale arises when a diffusing particle encounters random traps with a wide distribution of trapping times.[125-127] For the diffusional motion of polypeptide backbone sections, such random traps are caused by the wide range of native and non-native interactions present in a protein,[123,142,143] from the energetic cost of dihedral angle changes to attractive and repulsive forces between backbone and side chain groups as well as hydrophobic effects. These interactions cause the ruggedness of the potential energy landscape, Fig. 1, and hence can lead to the transient formation of a multitude of non-native conformations which are stabilised to different extent. The escape rate from a local conformation is governed by the depth of the corresponding well on the energy landscape, so that the hierarchical nature of this landscape, *i.e.* the wide range of well depths, yields a wide range of trapping times, as schematically shown in Fig. 1B.

More specifically, after disulfide bond photolysis the backbone can get trapped in a multitude of different conformations which hold the thiyl radicals apart from each other and thus prevent geminate recombination. The dispersion of trapping times of these conformations leads to the observed distribution of

geminate recombination times, which is much wider than expected from the normal diffusion that would occur in the absence of such trap dispersion. In fact, the unusual power law dependence of $k_{inst}(t) \sim t^{-0.94}$ over nine orders of magnitude in time can be shown to arise from such inhomogeneous trapping even when ignoring any separation of the radicals by diffusion. In the Supporting Information we describe a simplified model in which the radicals become trapped in close vicinity of each other immediately after bond photolysis and recombine upon escape from this trap. In this model, the assumption of a Gaussian depth distribution with a width of several k_BT is sufficient to yield $k_{inst}(t) \sim t^{-0.94}$ in the time range from pico- to milliseconds, see Fig. 8. This shows the importance of the trap dispersion for rationalizing our experimental results.

Thus, our results confirm that the hierarchical roughness of the energy landscape is relevant not only for small scale equilibrium fluctuations, as previously observed,[123,142,143] but also for large scale non-equilibrium conformational changes, including folding towards the native structure. The simulations of geminate recombination under subdiffusive conditions described above, Fig. 7, show that a value of ~ 0.3 is required for the subdiffusive parameter α to yield the experimentally observed time dependence of $k_{inst}(t) \sim t^{-0.94}$ over nine orders of magnitude in time. The distribution of jump activation energies E_j assumed in these simulations is $g(E_j) \sim \exp(-\alpha E_j/k_BT)$, so that $\alpha \sim 0.3$ corresponds to an exponential distribution of trap depths with a width of 3-4 k_BT. Previous reports in the literature determined the root-mean-squared trap depth, $\langle E_j^2 \rangle^{1/2}$, as a measure of the energy landscape roughness; this has a value of 4-5 k_BT for such an exponential distribution.

The energy landscape roughness of 4-5 k_BT inferred from the geminate recombination data, Fig. 5, is of a similar size as the values determined for proteins and bimolecular protein complexes by mechanical unfolding summarised above. This suggests that mechanical unfolding provides a reliable estimate of the energy landscape roughness, in spite of the various underlying assumptions discussed above and the possibility of an alternative interpretation of the experimental results.[98] On the other hand, roughness estimates from loop formation dynamics and folding studies yield somewhat smaller values, as detailed above. This may be partly due to the fact that some of these previous studies were undertaken on unstructured model peptides which had been designed to minimise residue-residue interactions. However, it also should be noted that most of these roughness estimates from loop formation experiments only provide lower limits for the roughness or are based on estimates of the speed of backbone diffusion in the absence of local interactions which are difficult to obtain with high accuracy.[92] Furthermore, all of the previously reported values for the roughness of the energy landscape are based on Zwanzig's theory of motion in a rough potential[89] which is limited to one dimension, and it is not clear how this limited dimensionality affects dynamic estimates for complex chain motions.[90,91] The roughness parameter obtained here does not suffer from any of these shortcomings.

It is instructive to compare the experimentally determined width of trap energies of 3-4 k_BT to the strengths of typical residue-residue interactions in proteins. The strength of van-der-Waals interactions in tightly packed crystals can reach values of up to 10 kJ/mol (~ 4 k_BT),[154] although somewhat smaller values are expected in less tightly packed proteins. Hydrogen bonds have typical strengths of 2-7 kJ/mol (~ 1-3 k_BT),[155] salt bridges contribute 2 kJ/mol (~ k_BT),[156] whereas π-π interactions and the hydrophobic effect between aromatic side chains can contribute up to 5 kJ/mol to protein stability (2 k_BT).[157] This suggests that many of the local traps are caused by individual interactions between a pair of residues. However, the tail end of the trap depth distribution is more likely to result from the cumulative effect of several interactions.

In any real system, a maximum well depth and hence maximum trapping time must exist. Full equilibration is only possible on time scales longer than this maximum trapping time and diffusional motion becomes normal on longer time scales.[120,127,147] The experimental observation that the power law $k_{inst}(t) \sim t^{-0.94}$ persists over the full experimental time window used here, *i.e.* up to 1 ms, indicates the existence of deep traps, *i.e.* conformations with an escape time larger than 1 ms, in N-PGK. This is not so surprising for the molten-globule like structure which N-PGK adopts at low denaturant concentrations (2 M urea),[32,106] for which trapping on the millisecond time scale has been observed in NMR experiments.[158] These traps provide an explanation for the NMR line broadening generally observed in molten globule states. However, the data show that such deep traps with millisecond trapping times also exist under unfolding conditions (8 M urea), although probably with lower population. This shows that the protein energy landscape is significantly rugged even under these conditions and that even the presence of large amounts of urea does not prevent relatively strong residue-residue interactions. These results confirm suggestions of residual interactions in unfolded proteins which had been concluded from the results of photo-CIDNP NOE[159] and paramagnetic enhancement NMR experiments[160] and from the unusual denaturant dependence of intrapolymer diffusion.[16] They are also in agreement with conclusions from loop formation experiments which show that internal friction disappears only at guanidinium chloride (GdmCl) concentrations above 6-8 M,[13,15,16,18,21,22,86] when taking into account the well-known fact that GdmCl is twice as effective as denaturant as is urea.[161]

Transient non-native interactions, as found here even in the presence of denaturant, may significantly contribute towards the efficiency of the protein folding process. They may help to temporarily reduce the conformational space accessible to the polypeptide and thus enhance the formation of native contacts, particularly between residues which initially are far from each other. This is particularly important when considering the nature of subdiffusive motion, which reduces the encounter probability of such residues on short time scales, as discussed above. The involvement of non-native contacts in increasing folding efficiency has been suggested previously, based on simulations[29,162] as well as mutation experiments,[163] and may be the reason for "abnormal" Φ-values.[162] The current results on significant interactions even in the presence of denaturants can be interpreted as further experimental evidence of these suggestions.

On the other hand, transient interactions also affect the speed of motion over the energy landscape and hence contribute to the so-called "speed limit of protein folding".[94,164] This "speed limit" usually refers to the rate of folding from a manifold of unfolded

states at high energy to a low-energy folded state on a *free* energy landscape that has been optimised to not have a significant activation barrier (so-called "downhill folding"); it has been established to be on the order of microseconds for small proteins.[165] Since folding corresponds to motion on the multidimensional landscape of Fig. 1, this "speed limit" is seriously affected by the roughness of the energy landscape, *i.e.* the transient trapping of the protein in conformations which are stabilised by non-native interactions. Thus, a way of characterising the folding landscape roughness will contribute to a better understanding of the concept of the "folding speed limit". The absence of significant intrapeptide interactions in the simple model peptides used in loop formation experiments, which results in reduced energy landscape roughness, also explains why estimates of the protein folding "speed limit" obtained from such experiments overestimate the possible maximum folding rates of real proteins.[10]

Conclusions and Outlook

Important progress has been made in investigating the dynamics of the unfolded – or partially folded – polypeptide backbone. Conceptually, conformational changes of the backbone can be described as motion on a multi-dimensional energy landscape with significant roughness caused by local interactions. Characterisation of this landscape, and in particular its roughness, is an important factor in understanding functional processes, ranging from ligand binding to protein folding.

Loop formation experiments suggest that in equilibrium the motion of backbone sections seems to be well described by the normal diffusion equation, with the diffusion constant reflecting landscape roughness. Extensive work has characterised many details of the backbone dynamics and the factors governing it. For example, it was found that particular amino acids only have a minor effect on the speed of backbone diffusion. Solvent friction could be separated from intra-peptide friction, which arises from the formation of transient interactions and thus is directly related to the energy landscape roughness. Denaturants were shown to significantly reduce internal friction, in particular for real protein sequences with many potential non-native interactions, and thus significantly speed up backbone diffusion. Estimates of the energy landscape roughness yield values of only 1-2 k_BT, which is somewhat less than values measured using mechanical unfolding methods.

Only recently, a different experimental approach was used to show that the motion of backbone sections in fact is not following normal diffusional behaviour. Unlike the loop formation experiments, this approach allows the observation of backbone dynamics far from equilibrium by making use of the UV-photolysis of an aromatic disulfide bond which initially constrains the backbone to a non-equilibrium conformation. Moreover, there is no inherent limit to the time scales accessible by the method. Geminate recombination of the thiyl radicals formed by UV-photolysis was shown to follow unusual dynamics which are incompatible with normal diffusion of the backbone, but can be well described by strongly subdiffusive motion. Such subdiffusive backbone motion in fact is expected for an energy landscape with a hierarchy of minima which cause trapping of the backbone in particular conformations with a wide range of escape times. A comparison of the experimental results with the predictions of the theory of geminate recombination in the presence of such traps yielded a landscape roughness of 4-5 k_BT, of similar magnitude as values obtained by mechanical unfolding methods.

It has to be pointed out that the initial reports on the use of the new experimental approach did not make full use of the method. In particular, none of the experimental results show the change from a time-dependent instantaneous rate constant, $k_{inst}(t)$, to a time-independent value at long times which is expected to occur upon equilibration. This shows that full conformational equilibration of unfolded proteins is significantly slower than expected so far from equilibrium loop formation experiments, although only lower limits for the equilibration times can be given from the current results. For the α-helical peptides, equilibration is shown to be slower than a few microseconds, whereas the results for N-PGK show that equilibration only occurs beyond 1 ms, even in the presence of 8 M urea, Fig. 5. Thus, it will be of great interest to extend the time scales of these experiments. There is no intrinsic time limit for the method, provided that the concentration of proteins and other radical quenchers is kept low enough to avoid unwanted radical reactions, so that experiments are only limited by the sensitivity for detecting the remaining thiyl radicals. Given the signal-to-noise which is achievable in transient absorbance measurements in the visible spectral region, this does not provide a significant limitation. Furthermore, the intrinsic rate of recombination can be further reduced by suitable modifications of the aromatic disulfide.[105] It will be highly interesting to study the variation of the full equilibration time scale with modification of the solvent conditions, *e.g.* the addition of denaturant, or the protein itself.

On shorter time scales, it will be interesting to apply the method to unstructured oligopeptides, such as those used in previous loop formation experiments. Because of the lack of interacting side chains, these peptides are expected to have an energy landscape with reduced roughness and thus a narrower distribution of trapping times. This should yield diffusive behaviour closer to normal diffusion, *i.e.* a larger value of the subdiffusive parameter α, and hence a different time dependence of the instantaneous rate constant, $k_{inst}(t)$, compare Fig. 7, as well as full equilibration on a shorter time scale. Quantification of the roughness from such experiments might lead to a better characterisation of the residual interactions which can be found in such simple peptides, for which unspecific backbone hydrogen bonds have been suggested to be the main type of interaction.[13]

Another fundamental aspect which should be addressed is the temperature dependence of the energy landscape roughness, which has been suggested to increase with temperature due to the increased strength of the hydrophobic effect.[23,27] This could be easily addressed by applying the new method to temperature-denatured protein in addition to denaturant-denatured protein at low temperature.

For more detailed investigations and their interpretation, these experiments will need to be complemented by further theoretical work. MD simulations show a power law dependence of k_{inst} which is in good agreement with the experimental results.[113] This provides the opportunity of understanding the effect at atomistic level. In particular, it may be interesting to investigate the effect

of roughness variations over the energy landscape, which has been suggested previously.[22] The new non-equilibrium method which starts from a cyclic backbone conformation does in principle allow the separate observation of the roughness of the landscape far from equilibrium, *i.e.* close to the initial cyclic conformation which dominates the initial recombination dynamics, and that closer to equilibrium, which becomes increasingly important at later times.

Acknowledgments

The authors would like to thank all their coworkers who contributed to the development and application of the thiyl geminate recombination method: W.F. DeGrado, E.A. Gooding, Y. Kholodenko, H.S.M. Lu, G.D. Reid, S. Dev, D.J. Shaw, and in particular the late R.M. Hochstrasser, in whose lab the method was first tested and who took a continued interest in this work. Some of this work was supported by grants from the NIH and BBSRC.

Notes and references

[a] *Department of Chemistry, University of Liverpool, Liverpool, L69 3BX, UK. E-mail:m.volk@liv.ac.uk*
[b] *School of Chemical and Biological Sciences, Queen Mary, University of London, London E1 4NS, UK.*
[c] *Department of Molecular Biology and Biotechnology, University of Sheffield, Sheffield S10 2TN, UK.*
[d] *Manchester Institute of Biotechnology, Manchester, M1 7DN, UK.*
[e] *Department of Chemistry, University of Sheffield, Sheffield S10 2TN, UK.*
[f] *School of Chemistry, University of Edinburgh, Edinburgh EH9 3JJ, UK.*

† Electronic Supplementary Information (ESI) available: 1. Subdiffusive behaviour of polymer segments in the Rouse and Zimm models; 2. Random walk simulations comparing normal and subdiffusive motion; 3. Inhomogeneous trap model of geminate recombination. See DOI: 10.1039/b000000x/

‡ In this Perspective article, the term "energy landscape" is referring to the full multidimensional landscape, *i.e.* the energy of the protein as a function of *all* coordinates. It should be noted that the concept of a folding funnel on such a multidimensional landscape is more a way of focussing thought about the process of folding than a detailed model which can be directly related to experimental or computational results. This is in contrast to low-dimensional landscape funnels which can be calculated from computational results using only a few relevant well-defined coordinates, such as *e.g.* the polypeptide end-to-end distance, the fraction of native contacts, or the root-mean square deviation of residue positions from the native structure. Unfortunately, any pictorial cartoon of the full folding landscape is also limited to two dimensions.

§ In this Perspective article, to avoid confusion, we reserve the word "diffusion" exclusively for diffusion of molecules or molecular groups in three-dimensional real space, and do not apply it to the concept of motion in multi-dimensional configurational space or motion along a one-dimensional reaction coordinate, which often also are described as "diffusional motion".

¶ The distance dependence of the quenching reaction has to be carefully considered for the analysis of the experimental results and for correct interpretation of the measured quenching rates. In the context of investigating loop formation during protein folding, the ideal reporter state and quencher should be chosen so that quenching occurs only upon van-der-Waals contact, which is the case for fluorescence quenching by hydrogen atom transfer or exciplex formation. Dexter-type energy transfer and electron-transfer induced quenching occur over only slightly larger distances, and so can still yield direct information on protein loop formation. Foerster-type energy transfer, which is the basis for Fluorescence Resonance Energy Transfer (FRET) experiments, on the other hand, can occur over larger distances of several tens of Ångstroms or more. Thus, FRET-detected single molecule correlation experiments are likely to yield a more general measure for (long-range) backbone reconfiguration dynamics rather than directly providing loop formation dynamics; on the other hand, they allow the direct measurement of end-to-end distance distributions.

‖ Non-geminate recombination can be ruled out based on the concentration of radicals and reasonable values of the diffusion constant of the peptides/N-PGK.

†† Conceptually, the strongly non-exponential radical concentration $c(t)$ could be described using an exponential with a time dependent rate constant $k(t)$, *i.e.* $c(t) \sim \exp(-k(t)*t)$ and $k_{inst}(t)$ is closely related to $k(t)$. If $k(t)$ has a power law time dependence, $k(t) \sim t^{-p}$, $k_{inst}(t) = (1-p)\,k(t)$, i.e. except for a trivial numerical factor the two quantities have the same time dependence. However, even for a time-dependent $c(t)$ which corresponds to a non-power law $k(t)$, $k_{inst}(t)$ is a direct measure for the fraction of radical pairs that is at the contact distance, and thus for the time dependence of the re-encounter probability of the two radicals.

‡‡ In the presence of a potential $U(\boldsymbol{x})$ which acts on the diffusing particle, this equation has to be extended to yield the Smoluchowski equation

$$\frac{\partial}{\partial t}p(\boldsymbol{x},t) = D\nabla^2 p(\boldsymbol{x},t) + D\nabla\left(p(\boldsymbol{x},t)\nabla U(\boldsymbol{x})/kT\right)$$

Although in this case the mean square displacement will not increase linearly with time, the motion is still referred to as "normal diffusion".

§§ Theoretically, free subdiffusion (*i.e.* subdiffusion in the absence of an external potential) can be shown to be described by an extension of the normal diffusion equation, Eq. (2):

$$\frac{\partial}{\partial t}p(\boldsymbol{x},t) = {}_0D_t^{1-\alpha} D_\alpha \nabla^2 p(\boldsymbol{x},t)$$

where D_α is a generalized diffusion coefficient with dimension $[D_\alpha] = \text{Å}^2\,\text{ns}^{-\alpha}$ and ${}_0D_t^{1-\alpha}$ is the Riemann-Liouville operator:

$${}_0D_t^{1-\alpha} f(\boldsymbol{x},t) = \frac{1}{\Gamma(\alpha)}\frac{\partial}{\partial t}\int_0^t dt' \frac{f(\mathrm{x},t')}{(t-t')^{1-\alpha}}$$

¶¶ In any real system, a maximum trapping time exists which is given by depth of the deepest trap(s) of the energy surface on which the particle moves. This is ignored in the current simulations which assume an exponential distribution of jump activation energies. Subdiffusive behaviour turns into normal diffusion on the time scale of the longest trapping times.

1 C. B. Anfinsen, *Science*, 1973, **181**, 223-230.
2 C. Levinthal, *J. Chim. Phys. Phys.-Chim. Biol.*, 1968, **65**, 44-45.
3 (a) A. Ansari, J. Berendzen, S. F. Bowne, H. Frauenfelder, I. E. T. Iben, T. B. Sauke, E. Shyamsunder and R. D. Young, *Proc. Natl. Acad. Sci. U.S.A.*, 1985, **82**, 5000-5004; (b) H. Frauenfelder, S. G. Sligar and P. G. Wolynes, *Science*, 1991, **254**, 1598-1603.
4 (a) H. Frauenfelder, F. Parak and R. D. Young, *Annu. Rev. Biophys. Biophys. Chem.*, 1988, **17**, 451-479; (b) R. L. Baldwin, *Nature*, 1994, **369**, 183-184; (c) P. G. Wolynes, J. N. Onuchic and D. Thirumalai, *Science*, 1995, **267**, 1619-1620; (d) J. D. Bryngelson, J. N. Onuchic, N. D. Socci and P. G. Wolynes, *Proteins: Struct., Funct., Genet.*, 1995, **21**, 167-195; (e) K. A. Dill and H. S. Chan, *Nat. Struct. Biol.*, 1997, **4**, 10-19; (f) J. N. Onuchic, Z. Luthey-Schulten and P. G. Wolynes, *Annu. Rev. Phys. Chem.*, 1997, **48**, 545-600; (g) J. N. Onuchic and P. G. Wolynes, *Curr. Opin. Struct. Biol.*, 2004, **14**, 70-75.
5 (a) A. Sali, E. Shakhnovich and M. Karplus, *Nature*, 1994, **369**, 248-251; (b) T. Lazaridis and M. Karplus, *Science*, 1997, **278**, 1928-1931; (c) M. Oliveberg and P. G. Wolynes, *Q. Rev. Biophys.*, 2005, **38**, 245-288.
6 H. Frauenfelder, P. W. Fenimore, G. Chen and B. H. McMahon, *Proc. Natl. Acad. Sci. U.S.A.*, 2006, **103**, 15469-15472.
7 P. E. Leopold, M. Montal and J. N. Onuchic, *Proc. Natl. Acad. Sci. U.S.A.*, 1992, **89**, 8721-8725.
8 M. Jacob and F. X. Schmid, *Biochemistry*, 1999, **38**, 13773-13779.
9 A. Ansari, C. M. Jones, E. R. Henry, J. Hofrichter and W. A. Eaton, *Science*, 1992, **256**, 1796-1798.

10 (a) S. J. Hagen, L. L. Qiu and S. A. Pabit, *J. Phys.: Condens. Matter*, 2005, **17**, S1503-S1514; (b) S. A. Pabit, H. Roder and S. J. Hagen, *Biochemistry*, 2004, **43**, 12532-12538.
11 S. J. Hagen, *Curr. Protein Pept. Sci.*, 2010, **11**, 385-395.
12 (a) J. M. Sorenson, G. Hura, A. K. Soper, A. Pertsemlidis and T. Head-Gordon, *J. Phys. Chem. B*, 1999, **103**, 5413-5426; (b) P. W. Fenimore, H. Frauenfelder, B. H. McMahon and F. G. Parak, *Proc. Natl. Acad. Sci. U.S.A.*, 2002, **99**, 16047-16051; (c) M. Chaplin, *Nat. Rev. Mol. Cell Biol.*, 2006, **7**, 861-866; (d) Y. Levy and J. N. Onuchic, *Annu. Rev. Biophys. Biomol. Struct.*, 2006, **35**, 389-415; (e) T. M. Raschke, *Curr. Opin. Struct. Biol.*, 2006, **16**, 152-159; (f) H. Frauenfelder, G. Chen, J. Berendzen, P. W. Fenimore, H. Jansson, B. H. McMahon, I. R. Stroe, J. Swenson and R. D. Young, *Proc. Natl. Acad. Sci. U.S.A.*, 2009, **106**, 5129-5134.
13 A. Möglich, K. Joder and T. Kiefhaber, *Proc. Natl. Acad. Sci. U.S.A.*, 2006, **103**, 12394-12399.
14 K. Chattopadhyay, E. L. Elson and C. Frieden, *Proc. Natl. Acad. Sci. U.S.A.*, 2005, **102**, 2385-2389.
15 D. Nettels, I. V. Gopich, A. Hoffmann and B. Schuler, *Proc. Natl. Acad. Sci. U.S.A.*, 2007, **104**, 2655-2660.
16 V. R. Singh, M. Kopka, Y. Chen, W. J. Wedemeyer and L. J. Lapidus, *Biochemistry*, 2007, **46**, 10046-10054.
17 Y. J. Chen, C. Parrini, N. Taddei and L. J. Lapidus, *J. Phys. Chem. B*, 2009, **113**, 16209-16213.
18 V. A. Voelz, V. R. Singh, W. J. Wedemeyer, L. J. Lapidus and V. S. Pande, *J. Am. Chem. Soc.*, 2010, **132**, 4702-4709.
19 Y. Chen, W. J. Wedemeyer and L. J. Lapidus, *J. Phys. Chem. B*, 2010, **114**, 15969-15975.
20 S. A. Waldauer, O. Bakajin and L. J. Lapidus, *Proc. Natl. Acad. Sci. U.S.A.*, 2010, **107**, 13713-13717.
21 V. A. Voelz, M. Jaeger, S. Yao, Y. Chen, L. Zhu, S. A. Waldauer, G. R. Bowman, M. Friedrichs, O. Bakajin, L. J. Lapidus, S. Weiss and V. S. Pande, *J. Am. Chem. Soc.*, 2012, **134**, 12565-12577.
22 A. Borgia, B. G. Wensley, A. Soranno, D. Nettels, M. B. Borgia, A. Hoffmann, S. H. Pfeil, E. A. Lipman, J. Clarke and B. Schuler, *Nat. Commun.*, 2012, **3**, 1195.
23 J. Sabelko, J. Ervin and M. Gruebele, *Proc. Natl. Acad. Sci. U.S.A.*, 1999, **96**, 6031-6036.
24 M. Sadqi, L. J. Lapidus and V. Munoz, *Proc. Natl. Acad. Sci. U.S.A.*, 2003, **100**, 12117-12122.
25 W. Y. Yang and M. Gruebele, *Biophys. J.*, 2004, **87**, 596-608.
26 T. Cellmer, E. R. Henry, J. Hofrichter and W. A. Eaton, *Proc. Natl. Acad. Sci. U.S.A.*, 2008, **105**, 18320-18325.
27 F. Liu, M. Nakaema and M. Gruebele, *J. Chem. Phys.*, 2009, **131**, 195101.
28 M. Karplus, *J. Phys. Chem. B*, 2000, **104**, 11-27.
29 (a) R. B. Best and G. Hummer, *Proc. Natl. Acad. Sci. U.S.A.*, 2010, **107**, 1088-1093; (b) R. B. Best and G. Hummer, *Phys. Chem. Chem. Phys.*, 2011, **13**, 16902-16911.
30 J. C. F. Schulz, L. Schmidt, R. B. Best, J. Dzubiella and R. R. Netz, *J. Am. Chem. Soc.*, 2012, **134**, 6273-6279.
31 W. A. Eaton, *Proc. Natl. Acad. Sci. U.S.A.*, 1999, **96**, 5897-5899.
32 L. Milanesi, J. P. Waltho, C. A. Hunter, D. J. Shaw, G. S. Beddard, G. D. Reid, S. Dev and M. Volk, *Proc. Natl. Acad. Sci. U.S.A.*, 2012, **109**, 19563-19568.
33 E. Haas, E. Katchalski-Katzir and I. Z. Steinberg, *Biopolymers*, 1978, **17**, 11-31.
34 C. M. Jones, E. R. Henry, Y. Hu, C. K. Chan, S. D. Luck, A. Bhuyan, H. Roder, J. Hofrichter and W. A. Eaton, *Proc. Natl. Acad. Sci. U.S.A.*, 1993, **90**, 11860-11864.
35 B. Schuler and H. Hofmann, *Curr. Opin. Struct. Biol.*, 2013, **23**, 36-47.
36 H. Neuweiler, A. Schulz, M. Bohmer, J. Enderlein and M. Sauer, *J. Am. Chem. Soc.*, 2003, **125**, 5324-5330.
37 D. Nettels, A. Hoffmann and B. Schuler, *J. Phys. Chem. B*, 2008, **112**, 6137-6146.
38 A. Hoffmann, D. Nettels, J. Clark, A. Borgia, S. E. Radford, J. Clarke and B. Schuler, *Phys. Chem. Chem. Phys.*, 2011, **13**, 1857-1871.
39 O. Bieri, J. Wirz, B. Hellrung, M. Schutkowski, M. Drewello and T. Kiefhaber, *Proc. Natl. Acad. Sci. U.S.A.*, 1999, **96**, 9597-9601.
40 L. J. Lapidus, P. J. Steinbach, W. A. Eaton, A. Szabo and J. Hofrichter, *J. Phys. Chem. B*, 2002, **106**, 11628-11640.
41 F. Huang and W. M. Nau, *Angew. Chem., Int. Edit.*, 2003, **42**, 2269-2272.
42 A. Möglich, F. Krieger and T. Kiefhaber, *J. Mol. Biol.*, 2005, **345**, 153-162.
43 L. J. Lapidus, W. A. Eaton and J. Hofrichter, *Proc. Natl. Acad. Sci. U.S.A.*, 2000, **97**, 7220-7225.
44 R. R. Hudgins, F. Huang, G. Gramlich and W. M. Nau, *J. Am. Chem. Soc.*, 2002, **124**, 556-564.
45 F. Krieger, B. Fierz, O. Bieri, M. Drewello and T. Kiefhaber, *J. Mol. Biol.*, 2003, **332**, 265-274.
46 F. Huang, R. R. Hudgins and W. M. Nau, *J. Am. Chem. Soc.*, 2004, **126**, 16665-16675.
47 F. Krieger, A. Moglich and T. Kiefhaber, *J. Am. Chem. Soc.*, 2005, **127**, 3346-3352.
48 F. Huang and W. M. Nau, *Res. Chem. Intermed.*, 2005, **31**, 717-726.
49 M. Buscaglia, L. J. Lapidus, W. A. Eaton and J. Hofrichter, *Biophys. J.*, 2006, **91**, 276-288.
50 H. Sahoo, A. Hennig and W. M. Nau, *Int. J. Photoenergy*, 2006, **2006**, 89638.
51 B. Fierz and T. Kiefhaber, *J. Am. Chem. Soc.*, 2007, **129**, 672-679.
52 B. Fierz, H. Satzger, C. Root, P. Gilch, W. Zinth and T. Kiefhaber, *Proc. Natl. Acad. Sci. U.S.A.*, 2007, **104**, 2163-2168.
53 H. Neuweiler, M. Lollmann, S. Doose and M. Sauer, *J. Mol. Biol.*, 2007, **365**, 856-869.
54 V. R. Singh and L. J. Lapidus, *J. Phys. Chem. B*, 2008, **112**, 13172-13176.
55 A. Soranno, R. Longhi, T. Bellini and M. Buscaglia, *Biophys. J.*, 2009, **96**, 1515-1528.
56 I. Daidone, H. Neuweiler, S. Doose, M. Sauer and J. C. Smith, *PLOS Comput. Biol.*, 2010, **6**, e1000645.
57 A. Szabo, K. Schulten and Z. Schulten, *J. Chem. Phys.*, 1980, **72**, 4350-4357.
58 D. Roccatano, H. Sahoo, M. Zacharias and W. M. Nau, *J. Phys. Chem. B*, 2007, **111**, 2639-2646.
59 (a) H. Jacobson and W. H. Stockmayer, *J. Chem. Phys.*, 1950, **18**, 1600-1606; (b) G. Wilemski and M. Fixman, *J. Chem. Phys.*, 1974, **60**, 878-890; (c) N. M. Toan, G. Morrison, C. Hyeon and D. Thirumalai, *J. Phys. Chem. B*, 2008, **112**, 6094-6106.
60 B. Friedman and B. O'Shaughnessy, *Macromolecules*, 1993, **26**, 4888-4898.
61 R. R. Cheng, T. Uzawa, K. W. Plaxco and D. E. Makarov, *Biophys. J.*, 2010, **99**, 3959-3968.
62 S. Bollmann, A. Burgert, C. Plattner, L. Nagel, N. Sewald, M. Loellmann, M. Sauer and S. Doose, *ChemPhysChem*, 2011, **12**, 2907-2911.
63 R. R. Cheng, A. T. Hawk and D. E. Makarov, *J. Chem. Phys.*, 2013, **138**, 074112.
64 D. P. Teufel, C. M. Johnson, J. K. Lum and H. Neuweiler, *J. Mol. Biol.*, 2011, **409**, 250-262.
65 (a) L. J. Lapidus, W. A. Eaton and J. Hofrichter, *J. Mol. Biol.*, 2002, **319**, 19-25; (b) S. Neumaier, A. Reiner, M. Buettner, B. Fierz and T. Kiefhaber, *Proc. Natl. Acad. Sci. U.S.A.*, 2013, **110**, 12905-12910.
66 B. Fierz, A. Reiner and T. Kiefhaber, *Proc. Natl. Acad. Sci. U.S.A.*, 2009, **106**, 1057-1062.
67 (a) S. Williams, T. P. Causgrove, R. Gilmanshin, K. S. Fang, R. H. Callender, W. H. Woodruff and R. B. Dyer, *Biochemistry*, 1996, **35**, 691-697; (b) T. Wang, Y. Zhu, Z. Getahun, D. Du, C.-Y. Huang, W. F. DeGrado and F. Gai, *J. Phys. Chem. B*, 2004, **108**, 15301-15310; (c) C.-Y. Huang, J. W. Klemke, Z. Getahun, W. F. DeGrado and F. Gai, *J. Am. Chem. Soc.*, 2001, **123**, 9235-9238; (d) P. A. Thompson, W. A. Eaton and J. Hofrichter, *Biochemistry*, 1997, **36**, 9200-9210.
68 E. A. Gooding, A. Pozo Ramajo, J. Wang, C. Palmer, E. Fouts and M. Volk, *Chem. Commun.*, 2005, 5985-5987.
69 S. A. Petty and M. Volk, *Phys. Chem. Chem. Phys.*, 2004, **6**, 1022-1030.
70 A. Pozo Ramajo, S. A. Petty, A. Starzyk, S. M. Decatur and M. Volk, *J. Am. Chem. Soc.*, 2005, **127**, 13784-13785.
71 A. Pozo Ramajo, S. A. Petty and M. Volk, *Chem. Phys.*, 2006, **323**, 11-20.

72 E. A. Gooding, S. Sharma, S. A. Petty, E. A. Fouts, C. J. Palmer, B. E. Nolan and M. Volk, *Chem. Phys.*, 2013, **422**, 115-123.
73 (a) D. R. Buckler, E. Haas and H. A. Scheraga, *Biochemistry*, 1995, **34**, 15965-15978; (b) S. J. Hagen, J. Hofrichter, A. Szabo and W. A. Eaton, *Proc. Natl. Acad. Sci. U.S.A.*, 1996, **93**, 11615-11617; (c) S. J. Hagen, J. Hofrichter and W. A. Eaton, *J. Phys. Chem. B*, 1997, **101**, 2352-2365; (d) E. Sherman and G. Haran, *ChemPhysChem*, 2011, **12**, 696-703.
74 S. J. Hagen, C. W. Carswell and E. M. Sjolander, *J. Mol. Biol.*, 2001, **305**, 1161-1171.
75 (a) M. Buscaglia, B. Schuler, L. J. Lapidus, W. A. Eaton and J. Hofrichter, *J. Mol. Biol.*, 2003, **332**, 9-12; (b) I. J. Chang, J. C. Lee, J. R. Winkler and H. B. Gray, *Proc. Natl. Acad. Sci. U.S.A.*, 2003, **100**, 3838-3840; (c) S. Mukhopadhyay, R. Krishnan, E. A. Lemke, S. Lindquist and A. A. Deniz, *Proc. Natl. Acad. Sci. U.S.A.*, 2007, **104**, 2649-2654.
76 M. Buscaglia, J. Kubelka, W. A. Eaton and J. Hofrichter, *J. Mol. Biol.*, 2005, **347**, 657-664.
77 J. C. Lee, H. B. Gray and J. R. Winkler, *J. Am. Chem. Soc.*, 2005, **127**, 16388-16389.
78 (a) J. C. Lee, B. T. Lai, J. J. Kozak, H. B. Gray and J. R. Winkler, *J. Phys. Chem. B*, 2007, **111**, 2107-2112; (b) J. K. Lum, H. Neuweiler and A. R. Fersht, *J. Am. Chem. Soc.*, 2012, **134**, 1617-1622.
79 H. Neuweiler, C. M. Johnson and A. R. Fersht, *Proc. Natl. Acad. Sci. U.S.A.*, 2009, **106**, 18569-18574.
80 S. M. Vaiana, R. B. Best, W.-M. Yau, W. A. Eaton and J. Hofrichter, *Biophys. J.*, 2009, **97**, 2948-2957.
81 (a) A. C. M. Ferreon, Y. Gambin, E. A. Lemke and A. A. Deniz, *Proc. Natl. Acad. Sci. U.S.A.*, 2009, **106**, 5645-5650; (b) A. Grupi and E. Haas, *J. Mol. Biol.*, 2011, **405**, 1267-1283.
82 H. Neuweiler, W. Banachewicz and A. R. Fersht, *Proc. Natl. Acad. Sci. U.S.A.*, 2010, **107**, 22106-22110.
83 A. Reiner, P. Henklein and T. Kiefhaber, *Proc. Natl. Acad. Sci. U.S.A.*, 2010, **107**, 4955-4960.
84 T. Cellmer, M. Buscaglia, E. R. Henry, J. Hofrichter and W. A. Eaton, *Proc. Natl. Acad. Sci. U.S.A.*, 2011, **108**, 6103-6108.
85 (a) B. Ahmad, Y. Chen and L. J. Lapidus, *Proc. Natl. Acad. Sci. U.S.A.*, 2012, **109**, 2336-2341; (b) B. Ahmad and L. J. Lapidus, *J. Biol. Chem.*, 2012, **287**, 9193-9199.
86 A. Soranno, B. Buchli, D. Nettels, R. R. Cheng, S. Mueller-Spaeth, S. H. Pfeil, A. Hoffmann, E. A. Lipman, D. E. Makarov and B. Schuler, *Proc. Natl. Acad. Sci. U.S.A.*, 2012, **109**, 17800-17806.
87 B. G. Wensley, S. Batey, F. A. C. Bone, Z. M. Chan, N. R. Tumelty, A. Steward, L. G. Kwa, A. Borgia and J. Clarke, *Nature*, 2010, **463**, 685-688.
88 G. Haran, *Curr. Opin. Struct. Biol.*, 2012, **22**, 14-20.
89 R. Zwanzig, *Proc. Natl. Acad. Sci. U.S.A.*, 1988, **85**, 2029-2030.
90 D. E. Makarov, *J. Chem. Phys.*, 2013, **138**, 014102.
91 R. R. Cheng and D. E. Makarov, *J. Chem. Phys.*, 2011, **134**, 085104.
92 J. J. Portman, *J. Chem. Phys.*, 2003, **118**, 2381-2391.
93 W. Y. Yang and M. Gruebele, *J. Am. Chem. Soc.*, 2004, **126**, 7758-7759.
94 W. Y. Yang and M. Gruebele, *Nature*, 2003, **423**, 193-197.
95 C. B. Hyeon and D. Thirumalai, *Proc. Natl. Acad. Sci. U.S.A.*, 2003, **100**, 10249-10253.
96 C. Hyeon and D. Thirumalai, *J. Phys.: Condens. Matter*, 2007, **19**, 113101.
97 R. Kapon, R. Nevo and Z. Reich, *Biochem. Soc. Trans.*, 2008, **36**, 1404-1408.
98 M. Schlierf and M. Rief, *J. Mol. Biol.*, 2005, **354**, 497-503.
99 H. Janovjak, H. Knaus and D. J. Muller, *J. Am. Chem. Soc.*, 2007, **129**, 246-247.
100 (a) R. Nevo, V. Brumfeld, R. Kapon, P. Hinterdorfer and Z. Reich, *EMBO Rep.*, 2005, **6**, 482-486; (b) F. Rico and V. T. Moy, *J. Mol. Recognit.*, 2007, **20**, 495-501; (c) J. Wakayama and S. Sugiyama, *Biochemistry*, 2012, **51**, 32-42.
101 J. Brujic, R. I. Hermans, K. A. Walther and J. M. Fernandez, *Nat. Phys.*, 2006, **2**, 282-286.
102 M. Volk, Y. Kholodenko, H. S. M. Lu, E. A. Gooding, W. F. DeGrado and R. M. Hochstrasser, *J. Phys. Chem. B*, 1997, **101**, 8607-8616.
103 M. Volk, *Eur. J. Org. Chem.*, 2001, 2605-2621.
104 C. Kolano, J. Helbing, G. Bucher, W. Sander and P. Hamm, *J. Phys. Chem. B*, 2007, **111**, 11297-11302.
105 H. S. M. Lu, M. Volk, Y. Kholodenko, E. Gooding, R. M. H. Hochstrasser and W. F. DeGrado, *J. Am. Chem. Soc.*, 1997, **119**, 7173-7180.
106 L. Milanesi, C. Jelinska, C. A. Hunter, A. M. Hounslow, R. A. Staniforth and J. P. Waltho, *Biochemistry*, 2008, **47**, 13620-13634.
107 G. H. Morine and R. R. Kuntz, *Chem. Phys. Lett.*, 1979, **67**, 552-554.
108 R. R. Lembke, L. V. Natarajan and R. R. Kuntz, *J. Photochem.*, 1983, **21**, 814-823.
109 N. A. Borisevich, N. A. Lysak, S. V. Melnichuk, S. A. Tikhomirov and G. B. Tolstorozhev, in *Ultrafast Phenomena in Spectroscopy*, ed. E. Klose and B. Wilhelmi, Springer, Berlin, Heidelberg, 1990, 276-281.
110 N. P. Ernsting, *Chem. Phys. Lett.*, 1990, **166**, 221-226.
111 T. W. Scott and S. N. Liu, *J. Phys. Chem.*, 1989, **93**, 1393-1396.
112 N. A. Borisevich, O. V. Buganov, V. L. Dubovskii, S. A. Tikhomirov and G. B. Tolstorozhev, *Opt. Spectrosc.*, 2005, **98**, 368-373.
113 D. V. Shalashilin, G. S. Beddard, E. Paci and D. R. Glowacki, *J. Chem. Phys.*, 2012, **137**, 165102.
114 K. J. Shin and R. Kapral, *J. Chem. Phys.*, 1978, **69**, 3685-3696.
115 T. Bultmann and N. P. Ernsting, *J. Phys. Chem.*, 1996, **100**, 19417-19424.
116 G. Wilemski and M. Fixman, *J. Chem. Phys.*, 1974, **60**, 866-877.
117 (a) D. K. Klimov and D. Thirumalai, *J. Mol. Biol.*, 2002, **317**, 721-737; (b) H. X. Zhou, *J. Phys. Chem. B*, 2001, **105**, 6763-6766; (c) M. S. Z. Kellermayer, S. B. Smith, H. L. Ganzier and C. Bustamante, *Science*, 1997, **276**, 1112-1116; (d) M. Rief, M. Gautel, A. Schemmel and H. E. Gaub, *Biophys. J.*, 1998, **75**, 3008-3014; (e) K. Wang, J. G. Forbes and A. J. Jin, *Prog. Biophys. Mol. Biol.*, 2001, **77**, 1-44.
118 (a) H. Yamakawa and W. H. Stockmayer, *J. Chem. Phys.*, 1972, **57**, 2843-2854; (b) O. Kratky and G. Porod, *Recl. Trav. Chim. Pays-Bas*, 1949, **68**, 1106-1122.
119 (a) D. S. Banks and C. Fradin, *Biophys. J.*, 2005, **89**, 2960-2971; (b) J. A. Dix and A. S. Verkman, *Annu. Rev. Biophys.*, 2008, **37**, 247-263; (c) M. R. Horton, F. Höfling, J. O. Rädler and T. Franosch, *Soft Matter*, 2010, **6**, 2648-2656.
120 Q. Xu, L. Feng, R. Sha, N. C. Seeman and P. M. Chaikin, *Phys. Rev. Lett.*, 2011, **106**, 228102.
121 A. Paciaroni, E. Cornicchi, M. Marconi, A. Orecchini, C. Petrillo, M. Haertlein, M. Moulin and F. Sacchetti, *J. R. Soc. Interface*, 2009, **6**, S635-S640.
122 (a) P. Senet, G. G. Maisuradze, C. Foulie, P. Delarue and H. A. Scheraga, *Proc. Natl. Acad. Sci. U.S.A.*, 2008, **105**, 19708-19713; (b) Y. Cote, P. Senet, P. Delarue, G. G. Maisuradze and H. A. Scheraga, *Proc. Natl. Acad. Sci. U.S.A.*, 2010, **107**, 19844-19849; (c) Y. Cote, P. Senet, P. Delarue, G. G. Maisuradze and H. A. Scheraga, *Proc. Natl. Acad. Sci. U.S.A.*, 2012, **109**, 10346-10351.
123 H. Yang, G. Luo, P. Karnchanaphanurach, T. M. Louie, I. Rech, S. Cova, L. Xun and X. S. Xie, *Science*, 2003, **302**, 262-266.
124 W. Min, G. Luo, B. J. Cherayil, S. C. Kou and X. S. Xie, *Phys. Rev. Lett.*, 2005, **94**, 198302.
125 E. Barkai, R. Metzler and J. Klafter, *Phys. Rev. E*, 2000, **61**, 132-138.
126 R. Metzler and J. Klafter, *Phys. Rep.*, 2000, **339**, 1-77.
127 R. Metzler and J. Klafter, *J. Phys. A-Math. Gen.*, 2004, **37**, R161-R208.
128 P. G. deGennes, *Physics*, 1967, **3**, 37-45.
129 A. Baumgärtner, *J. Chem. Phys.*, 1980, **72**, 871-879.
130 M. Doi and S. F. Edwards, *The Theory of Polymer Dynamics*, Clarendon Press, Oxford, 1986
131 G. S. Grest and K. Kremer, *Phys. Rev. A*, 1986, **33**, 3628-3631.
132 V. A. Harmandaris, V. G. Mavrantzas, D. N. Theodorou, M. Kröger, J. Ramirez, H. C. Öttinger and D. Vlassopoulos, *Macromolecules*, 2003, **36**, 1376-1387.
133 D. Panja, *J. Stat. Mech.: Theory Exp.*, 2010, L02001.
134 (a) P. R. Rouse, *J. Chem. Phys.*, 1953, **21**, 1272-1280; (b) B. H. Zimm, *J. Chem. Phys.*, 1956, **24**, 269-278.
135 R. Shusterman, S. Alon, T. Gavrinyov and O. Krichevsky, *Phys. Rev. Lett.*, 2004, **92**, 048303.

136 E. P. Petrov, T. Ohrt, R. G. Winkler and P. Schwille, *Phys. Rev. Lett.*, 2006, **97**,
137 K. Kremer and K. Binder, *J. Chem. Phys.*, 1984, **81**, 6381-6394.
138 P. R. Rouse, *J. Chem. Phys.*, 1953, **21**, 1272-1280.
139 P. H. Verdier, *J. Chem. Phys.*, 1966, **45**, 2118-2121.
140 B. S. Khatri and T. C. B. McLeish, *Macromolecules*, 2007, **40**, 6770-6777.
141 D. E. Makarov, *J. Chem. Phys.*, 2010, **132**, 035104.
142 G. Luo, I. Andricioaei, X. S. Xie and M. Karplus, *J. Phys. Chem. B*, 2006, **110**, 9363-9367.
143 A. E. Garcia and G. Hummer, *Proteins Struct. Funct. Genet.*, 1999, **36**, 175-191.
144 K. Seki, M. Wojcik and M. Tachiya, *J. Chem. Phys.*, 2003, **119**, 7525-7533.
145 G. Guigas and M. Weiss, *Biophys. J.*, 2008, **94**, 90-94.
146 M. J. Saxton, *Biophys. J.*, 1996, **70**, 1250-1262.
147 M. J. Saxton, *Biophys. J.*, 2007, **92**, 1178-1191.
148 F. Krieger, B. Fierz, F. Axthelm, K. Joder, D. Meyer and T. Kiefhaber, *Chem. Phys.*, 2004, **307**, 209-215.
149 L. J. Lapidus, *Curr. Opin. Struct. Biol.*, 2013, **23**, 30-35.
150 D. Baker, *Nature*, 2000, **405**, 39-42.
151 D. E. Shaw, P. Maragakis, K. Lindorff-Larsen, S. Piana, R. O. Dror, M. P. Eastwood, J. A. Bank, J. M. Jumper, J. K. Salmon, Y. Shan and W. Wriggers, *Science*, 2010, **330**, 341-346.
152 R. Metzler, E. Barkai and J. Klafter, *Phys. Rev. Lett.*, 1999, **82**, 3563-3567.
153 S. C. Kou, *Annals Appl. Stat.*, 2008, **2**, 501-535.
154 J. Caillet and P. Claverie, *Acta Crystallogr., Sect. A*, 1975, **31**, 448-461.
155 A. R. Fersht, *Trends Biochem. Sci.*, 1987, **12**, 301-304.
156 A. Horovitz, L. Serrano, B. Avron, M. Bycroft and A. R. Fersht, *J. Mol. Biol.*, 1990, **216**, 1031-1044.
157 L. Serrano, M. Bycroft and A. R. Fersht, *J. Mol. Biol.*, 1991, **218**, 465-475.
158 M. J. Cliff, C. J. Craven, J. P. Marston, A. M. Hounslow, A. R. Clarke and J. P. Waltho, *J. Mol. Biol.*, 2009, **385**, 266-277.
159 K. H. Mok, T. Nagashima, I. J. Day, P. J. Hore and C. M. Dobson, *Proc. Natl. Acad. Sci. U.S.A.*, 2005, **102**, 8899-8904.
160 D. J. Felitsky, M. A. Lietzow, H. J. Dyson and P. E. Wright, *Proc. Natl. Acad. Sci. U.S.A.*, 2008, **105**, 6278-6283.
161 J. K. Myers, C. N. Pace and J. M. Scholtz, *Protein Sci.*, 1995, **4**, 2138-2148.
162 L. Li, L. A. Mirny and E. I. Shakhnovich, *Nat. Struct. Biol.*, 2000, **7**, 336-342.
163 A. R. Viguera, C. Vega and L. Serrano, *Proc. Natl. Acad. Sci. U.S.A.*, 2002, **99**, 5349-5354.
164 J. Kubelka, J. Hofrichter and W. A. Eaton, *Curr. Opin. Struct. Biol.*, 2004, **14**, 76-88.
165 M. B. Prigozhin and M. Gruebele, *Phys. Chem. Chem. Phys.*, 2013, **15**, 3372-3388.